Renal Biopsy:
Clinical Correlations

AMERICAN SOCIETY OF NEPHROLOGY · ASN ·

KIDNEY WEEK 2024

October 23–27 | San Diego, CA

Case 1 from Jonathan E. Zuckerman MD, PhD, University of California Los Angeles

A 31-year-old Native American man has a history of ESKD due to Alport syndrome. He received his first kidney transplant at age 14 with allograft failure within one year, which reportedly failed due to non-compliance with medication. His second transplant at age 18 lasted three months and reportedly failed due to antibody-mediated rejection. He had been on dialysis for the past 10 years. His Calculated Panel Reactive Antibody (cPRA) was 100%. He received a third transplant from a deceased donor. Warm ischemic time was 20 minutes. Induction with anti-thymoglobulin. Maintenance immunosuppression included tacrolimus and mycophenolate mofetil. His post-transplant course was complicated by delayed graft function requiring hemodialysis due to hyperkalemia. He was making over one to two liters per day of urine. His baseline serum creatinine was not yet established, and the lowest measurement was 1.8 mg/dl. After approximately one month post-transplant, he was found to have increasing serum creatinine (2.8 mg/dL) as well as an increased urine protein to creatinine ratio (1.4 g/g). Given the high immunologic risk, there was a clinical concern for rejection. A kidney biopsy was performed.

Biopsy #1:

Light Microscopy:

Periodic Acid Schiff (PAS) stained sections:

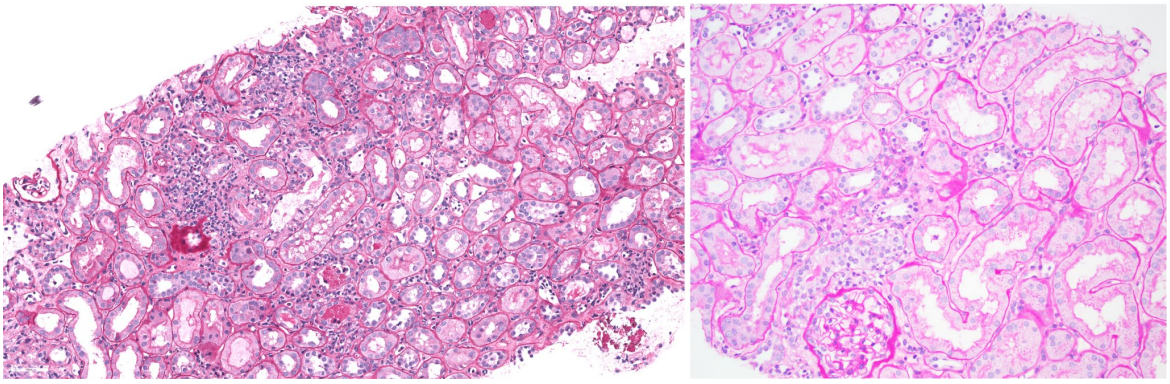

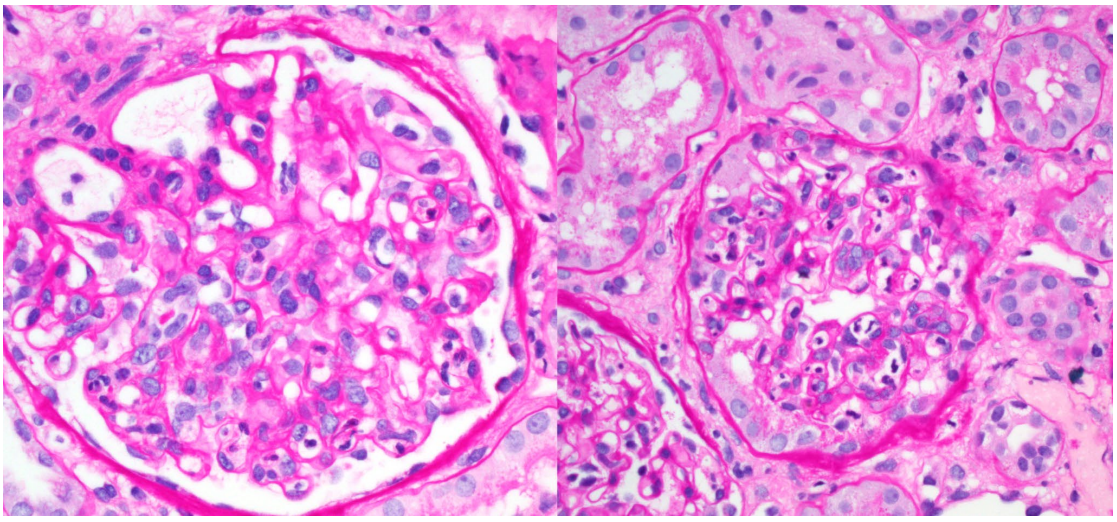

Jones Silver stained sections:

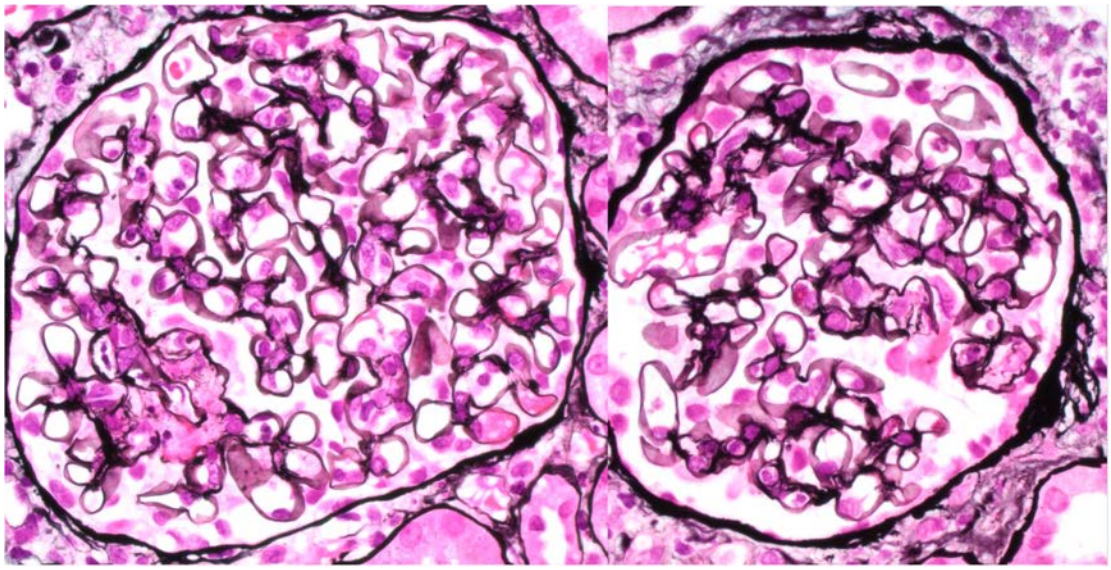

Immunofluorescence Microscopy:

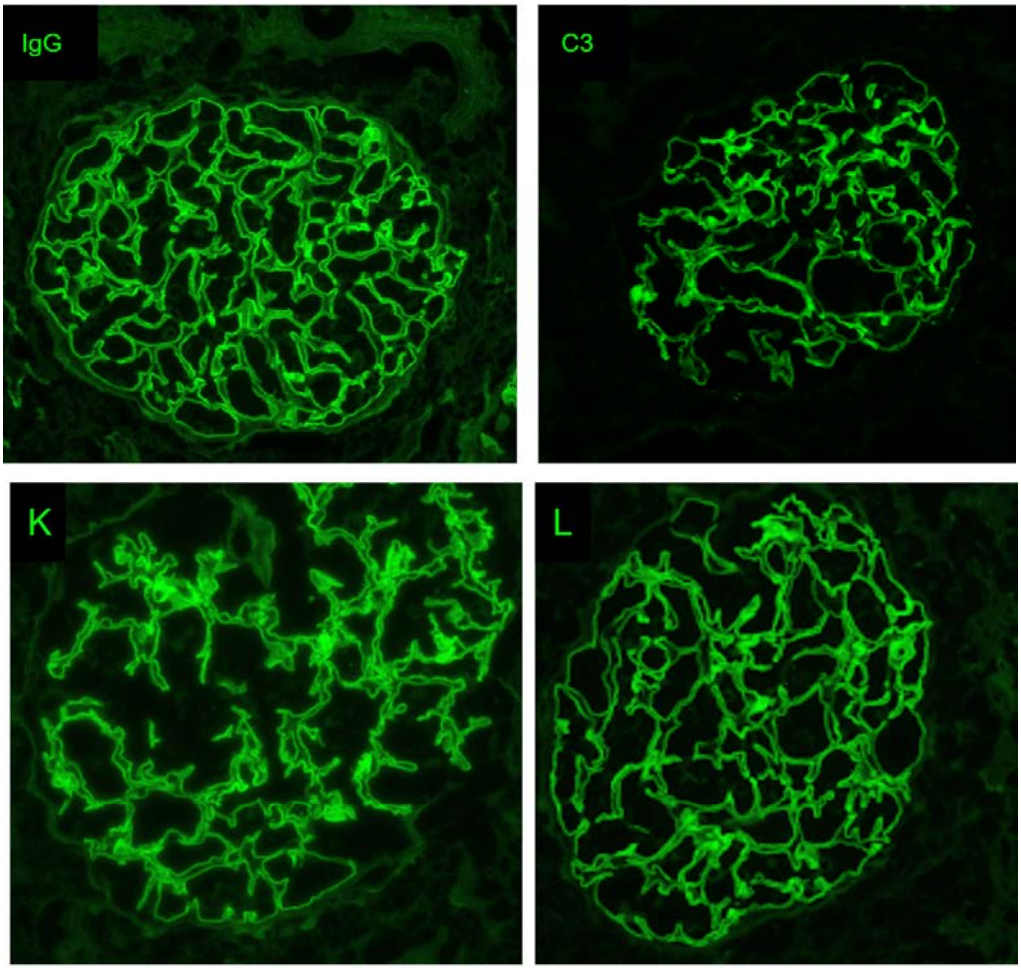

Electron Microscopy:

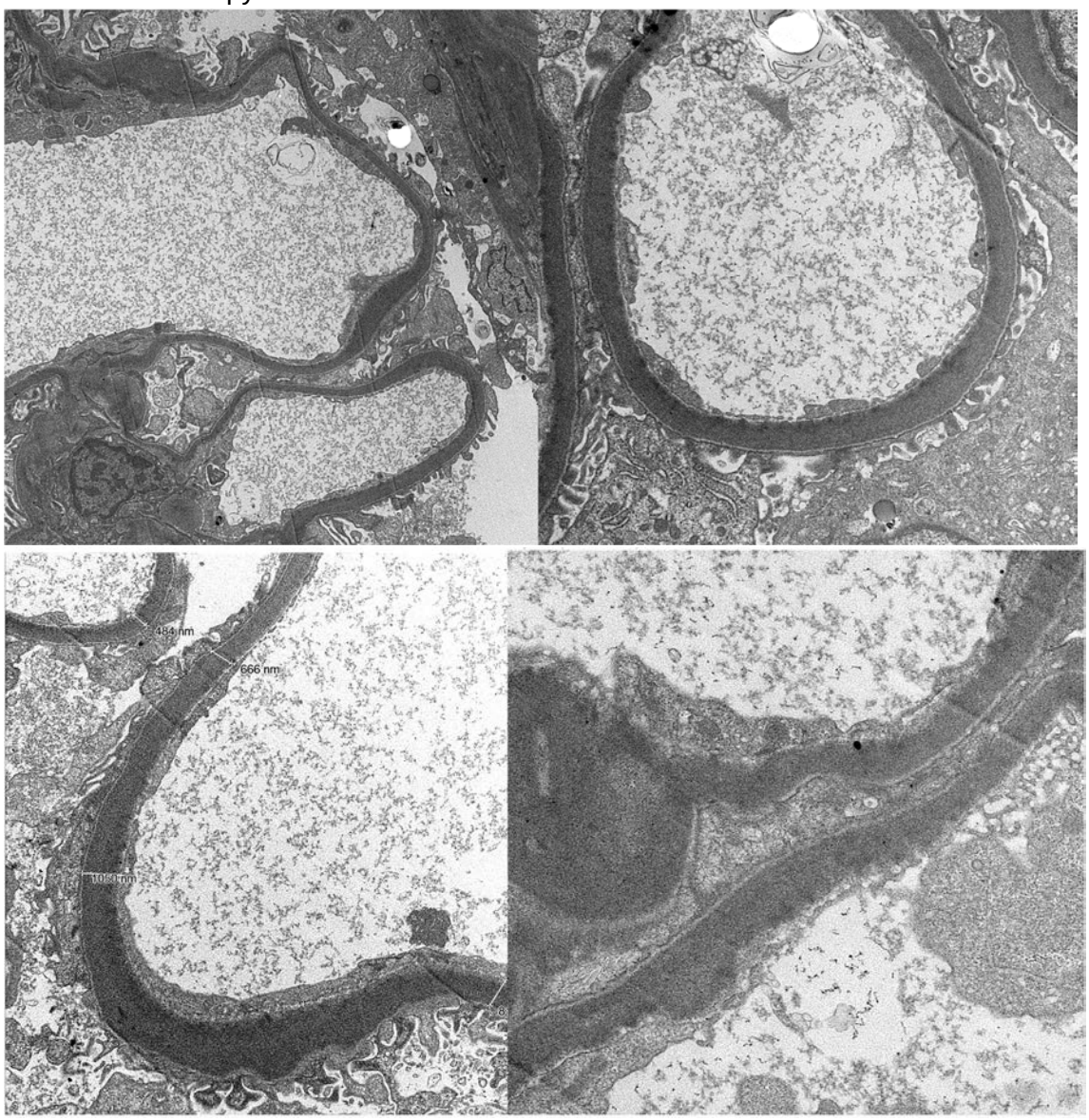

The patient had a second biopsy approximately one month later, as kidney function did not improve after treatment for the findings in the first biopsy.

Biopsy #2:
Light Microscopy:
PAS and Jones silver stained sections:

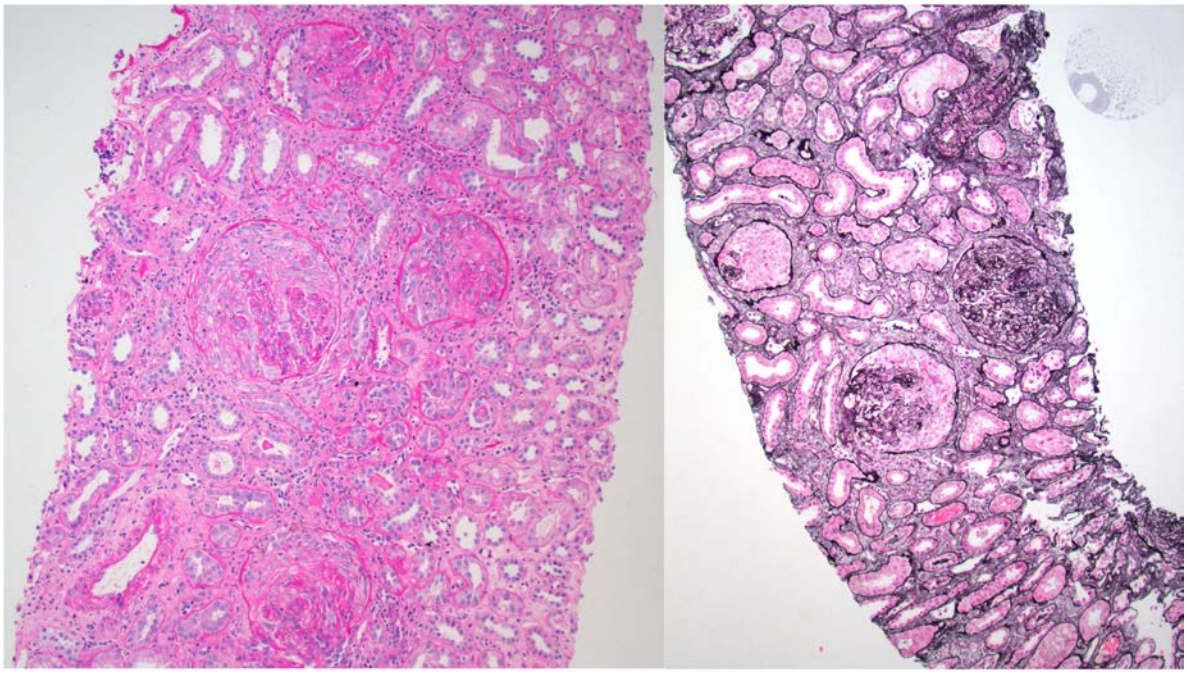

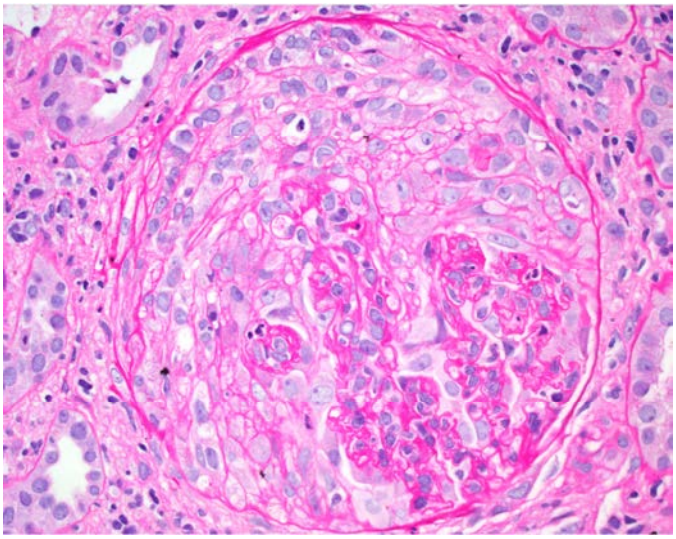

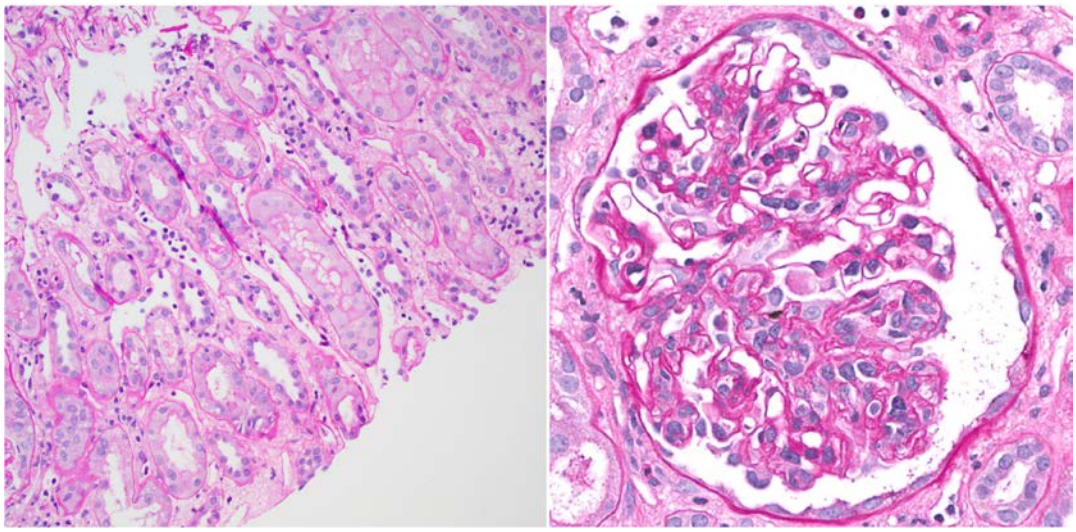

Immunofluorescence Microscopy:

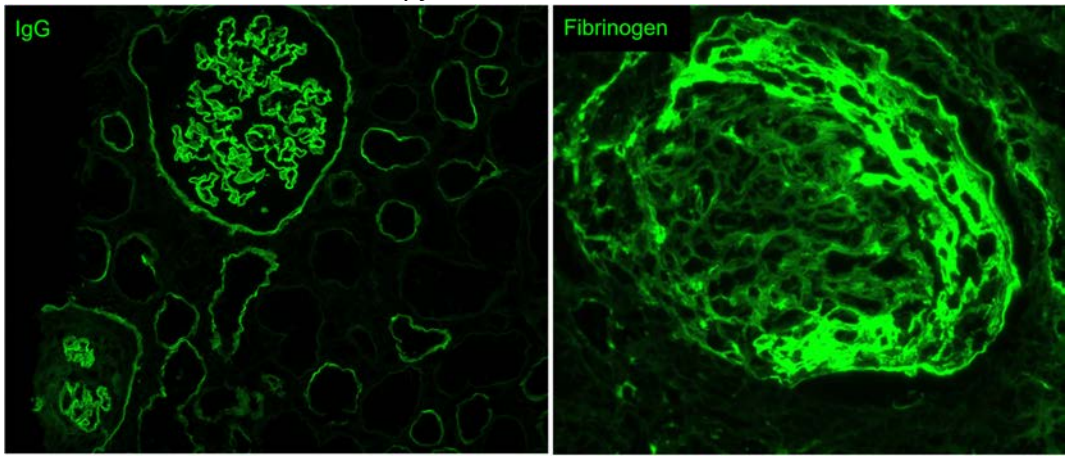

Electron Microscopy:

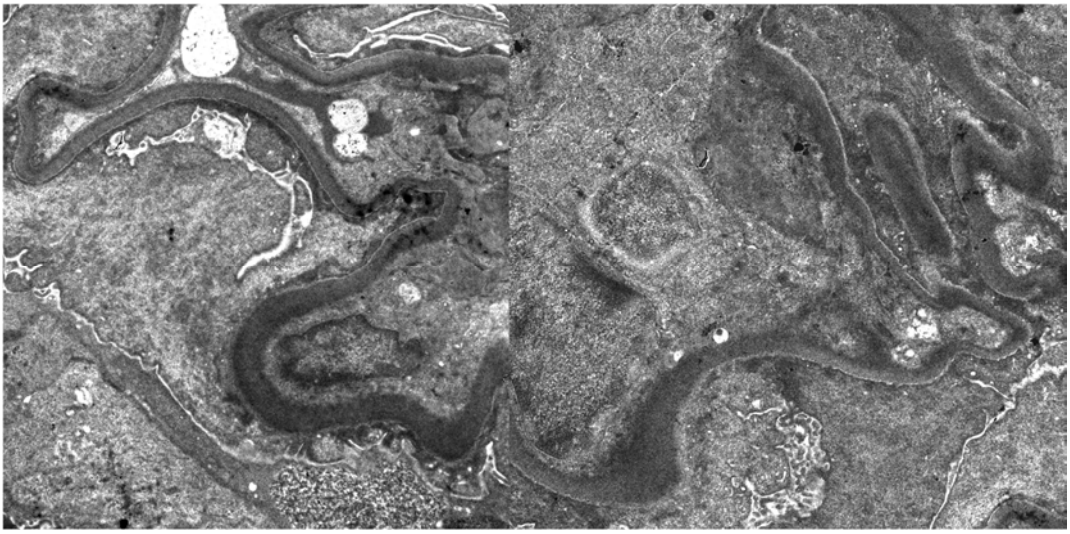

Pathologic Findings (Biopsy #1)

Light Microscopy: The specimen consists of three cores of cortex containing 34 non-sclerotic glomeruli and four arteries. Two glomeruli exhibit segmental, very early necrotizing lesions represented by breaks in the glomerular basement membrane (GBM) with minimal fibrin accumulation. No well-developed crescents are present. Many glomeruli exhibit segmental glomerulitis. There is patchy interstitial inflammation associated with focal mild to moderate tubulitis. There is patchy interstitial edema and acute tubular injury. There is patchy mild to moderate peritubular capillaritis. An SV40 stain is negative.

Banff scores:
g2, t2, i2, i-IFTA 0, t-IFTA-0, ti2, v0, ptc2, cg0, mm0, ct0,ci0, cv0, ah0

Immunofluorescence Microscopy: Frozen sections contain renal cortical tissue with 12 glomeruli, non-globally sclerotic. C4d is negative in peritubular capillaritis. GBMs exhibit diffuse and global linear staining for IgG (4+), C3 (4+), kappa (3+) and lambda (3+) light-chains. There is no other significant glomerular or tubulointerstitial staining.

Electron Microscopy: Toluidine blue-stained semi-thin sections contain renal cortical tissue containing three non-sclerotic glomeruli. Podocytes exhibit patchy mild foot process effacement (less than 10% of surface areas). GBMs show highly osmiophilic electron dense transformation and thickening as well as segmental subendothelial powdery electron dense deposits. Endothelial cells are closely applied to basement membranes and show variable swelling. Mesangial regions are normal in contour and cellularity. An occasional capillary loop lumen shows increased luminal leukocytes. Mesangial regions are normal in caliber and cellularity. There are no tubuloreticular inclusions. Peritubular capillaries basement membranes are normal.

Diagnosis and Interpretation (Biopsy #1)

- De novo anti-GBM antibody disease with rare focal segmental glomerular necrosis
- At least moderate microvascular inflammation ([g + ptc] >2) without C4d deposition, suggestive of C4d-negative active antibody-mediated rejection (correlation with donor specific antibodies is required for definitive diagnosis of antibody-mediated rejection)
- Acute T-cell-mediated rejection: IA, tubulointerstitial type

Pathologic Findings (Biopsy #2)

Light Microscopy: The specimen consists of seven cores of renal tissue composed of cortex, medulla, corticomedullary junction containing at least 55 glomeruli (10 globally sclerotic) and 10 arteries. About 32 glomeruli exhibit cellular to fibrocellular crescent formation. Many crescents are large and global. Some capillary loops exhibit fresh necrosis. Most of the globally sclerotic glomeruli exhibit features suggestive of old fibrous crescents. There is variable endocapillary hypercellularity, generally associated with crescents, but occasionally in areas away from crescent formation. Tubules exhibit features of acute injury, including epithelial cell attenuation, loss of brush border staining, epithelial cell sloughing, and reactive nuclear changes. There is

patchy interstitial inflammation composed of lymphocytes, histiocytes, and plasma cells. There is patchy moderate peritubular capillaritis.

Banff scores:
g2, t2, i2, i-IFTA 0, t-IFTA-0, ti2, v0, ptc2, cg0, mm0, ct0, ci0, cv0, ah0

Immunofluorescence Microscopy: Frozen sections contain renal cortical tissue with eight glomeruli. There is diffuse global linear glomerular capillary loop staining with IgG (4+), C3 (4+), kappa (4+), and lambda (4+) light-chains. Some tubular basement membranes exhibit linear tubular basement membrane staining with IgG, as do Bowman's capsules. At least four glomeruli were involved by crescents (highlighted by fibrinogen immunofluorescence).

Electron Microscopy: Toluidine blue-stained semi-thin sections contain renal cortical tissue containing one non-sclerotic glomerulus involved by a cellular crescent. Podocytes exhibit extensive foot process effacement. GBMs show highly osmiophilic electron dense transformation and thickening as well as segmental subendothelial powdery electron dense deposits. A few segments of GBM rupture are present. Endothelial cells show variable swelling. Mesangial regions are normal in contour and cellularity. A few capillary loop lumens show increased luminal leukocytes. Focal tubular basement membranes are thickened with possible powdery electron dense deposits.

Diagnosis and Interpretation (Biopsy #2)

- De novo anti-GBM antibody disease, severely active with early chronicity
    - Pattern of injury: diffuse necrotizing/crescentic and focal sclerosing glomerulonephritis with ~58% glomeruli involved by active cellular to fibrocellular crescents
- At least moderate microvascular inflammation ([g + ptc] >2) without C4d deposition and positive donor specific antibodies consistent with ongoing C4d-negative active antibody-mediated rejection (correlation with donor specific antibodies is required for definitive diagnosis of antibody-mediated rejection)
- Patchy tubulointerstitial inflammation, favor secondary to the glomerulonephritis, cannot rule out acute T-cell mediated rejection

Clinical Follow-Up

After the first biopsy, therapy was initiated, including anti-thymoglobulin (2.5 doses), pulse dose steroids (x11), IVIG, and mycophenolate mofetil was switched to cyclophosphamide. Anti-GBM titers after biopsy were found to range from eight to 21. Kidney function continued to deteriorate, and the patient required intermittent hemodialysis. HLA donor-specific antibodies to B44 and B49, as well as low-risk DSA to A11, were detected. The patient was also later found to develop positive cw16 DSA.

Following the second biopsy, anti-GBM titres were found to be increased to 28. Plasmapheresis was initiated for seven days with a drop in anti-GBM titers to 11. Urinary output increased from 200 cc to 500 cc per day. Rituximab treatment was also started after seven days of

plasmapheresis. He was subsequently on plasmapheresis three times per week as well as ongoing hemodialysis three times per week. An attempt was made to obtain imlifidase, but it was unavailable in the United States at that time. The patient ultimately had ongoing allograft failure despite treatment.

Between the first and second biopsies, the prior allograft nephrectomy pathology results were obtained, which indicated evidence of anti-GBM disease in the prior allograft kidneys.

Questions for Case 1

1. **How do you interpret the immunofluorescence microscopy findings from both biopsies?**

    A. Finely granular capillary wall staining for IgG
    B. Linear capillary wall staining for IgG
    C. Coarse granular capillary wall staining for IgG
    D. Granular mesangial staining for IgG
    E. Negative immunofluorescence staining

    The immunofluorescence studies show (B) global strong linear staining for IgG diagnostic for anti-GBM disease. (A,C,D) The staining is entirely smooth; no punctate granular staining is seen. Only the capillary walls are staining; mesangial regions are negative. (E) The bright green color in the image indicates a positive staining result.

2. **All but which one of the following diseases can result in immunofluorescence findings similar to the above case?**

    A. Diabetic nephropathy
    B. Membranous nephropathy
    C. Anti-GBM disease
    D. Monoclonal immunoglobulin deposition disease
    E. Pauci-immune necrotizing/crescentic glomerulonephritis

    (E) Pauci-immune glomerulonephritis should have negative or minimal immuno-fluorescence staining; strong positive immunofluorescence staining rules out this possibility. (A) Diabetic nephropathy may show non-specific pseudolinear staining of glomerular walls with IgG, as well as albumin, and can mimic anti-GBM disease. (B) Membranous nephropathy typically shows global granular capillary wall staining for IgG by immunofluorescence; however, deposits are occasionally confluent and can appear almost linear and mimic anti-GBM disease. (C) As noted in question #1, the image pictured is diagnostic for anti-GBM disease. (D) Monoclonal immunoglobulin deposition disease (heavy chain or heavy and light-chain type) can show linear glomerular capillary wall staining.

3. What is the major glomerular light microscopy pattern of injury in the second biopsy?

A. Glomerulitis
B. Membranous glomerulonephritis
C. Necrotizing/crescentic glomerulonephritis
D. Nodular mesangial sclerosis
E. Membranoproliferative glomerulonephritis

(C) The glomeruli are involved by numerous large cellular crescents, indicating a necrotizing/crescentic glomerulonephritis. (A) Some glomerulitis was present in this case; however, this was not the major finding and would not explain the crescents. (B) No capillary wall spikes or lucencies suggestive of membranous nephropathy were present in these images. (D) No mesangial sclerosis was present. (E) No capillary wall double contours were present, and the glomeruli did not show a lobulated appearance.

Discussion

De novo anti-GBM nephritis after transplantation in patients with Alport syndrome (AS) is reported to occur in 3% to 5% of men with AS who have undergone transplantation historically. More recent data suggest current incidence is lower (0.4-2.4%)[1,2,3]. Decreasing incidence has been attributed to modern potent immunosuppressive regimens (calcineurin inhibitors and mycophenolate mofetil). Acute rejection episodes(s) are common in reported cases (~70%) further supporting the idea that underimmunosuppression is a risk factor for this disease[1].

Most cases occur within the first year after transplant; however, some cases may be delayed (up to six years) and can recur in subsequent transplants[3]. Recurrence risk in re-transplanted patients is very high regardless of time interval since prior transplant(s) or the absence of detectable antibodies in circulation[4].

Most patients with de novo anti-GBM post transplantation are men with X-linked AS due to severe COL4A5 mutations, such as large deletions or large rearrangements. Following transplant, the wild type COL4A5 protein in the allograft basement membranes is recognized as foreign due to the absence of the alpha345 (IV) trimmers in the patient's native GBMs[5]. The antibodies formed are typically different from conventional anti-GBM disease, and thus anti-GBM serologic testing may be negative in these patients. In de novo anti-GBM disease, alloantibodies are formed against exposed quaternary epitopes of NC1 domains of intact α345NC1 (hexamer of α-3, α-4, or α-5 chains of collagen IV) rather than an exposed hidden epitope of the NC domain in conventional anti-GBM disease. Not all patients with severe COL4A5 mutations develop de novo anti-GBM after transplantation, and thus, other factors such as under immunosuppression may be involved in the pathogenesis.

The biopsy findings in de novo anti-GBM disease are similar to anti-GBM disease in the native kidney. Typically, >80% of glomeruli are involved by cellular crescents and/or necrotizing lesions. Associated tubular injury and red blood cell casts are present. Concurrent rejection has been reported. Immunofluorescence studies show strong linear IgG staining of GBMs as well as

Bowman's capsule and distal tubular basement membranes to varying degrees. The IgG deposition is polyclonal, and the areas of IgG staining will also show staining for kappa and lambda light-chains. C3 staining in a similar pattern may also be seen. Electron microscopic studies may show disrupted GBMs, crescent formation, and fibrin accumulation; however, electron dense deposits are not present[6].

The above case is unique in that there is electron-dense transformation and thickening of the lamina densa of the GBMs, and subendothelial deposits similar to those seen in monoclonal immunoglobulin deposition disease were observed. Such findings have not been reported in this setting to date and most likely reflect the heavy IgG deposition in this patient's basement membranes in the setting of a third transplant, resulting in exacerbation of this patient's pre-existing antibody response.

Interestingly, a subset of Alport patients have been characterized to develop linear IgG staining of GBMs without histologic features of glomerulonephritis[7]. This type of IgG staining is typically not associated with adverse graft outcomes nor associated with subsequent development of anti-GBM glomerulonephritis. This staining may disappear on follow-up biopsies.

Cases with very early mild glomerular lesions have been reported with progression to a frank necrotizing/crescentic glomerulonephritis over the course of several weeks[4]. Thus, even very focal early glomerulonephritis should be considered as significant anti-GBM disease. Such early lesions should be carefully sought in such cases, including additional levels as appropriate. Routine IgG immunofluorescence staining in all Alport patient biopsies after transplant should also be considered.

References

1. Byrne, M. C., Budisavljevic, M. N., Fan, Z., Self, S. E. & Ploth, D. W. Renal transplant in patients with Alport's syndrome. *Am. J. Kidney Dis.* 39, 769–775 (2002).
2. Peten, E. *et al.* Outcome of thirty patients with Alport's syndrome after renal transplantation. *Transplantation* 52, 823–826 (1991).
3. Gillion, V. *et al.* Genotype and Outcome After Kidney Transplantation in Alport Syndrome. *Kidney Int Rep* 3, 652–660 (2018).
4. Browne, G. *et al.* Retransplantation in Alport post-transplant anti-GBM disease. *Kidney Int.* 65, 675–681 (2004).
5. Olaru, F. *et al.* Quaternary epitopes of α345(IV) collagen initiate Alport post-transplant anti-GBM nephritis. *J. Am. Soc. Nephrol.* 24, 889–895 (2013).
6. Seshan, S. V. & Salvatore, S. P. De novo Glomerular Disease and the Significance of Electron Microscopy in Renal Transplantation. *Glomerular Dis* 1, 160–172 (2021).
7. Quérin, S. *et al.* Linear glomerular IgG fixation in renal allografts: incidence and significance in Alport's syndrome. *Clin. Nephrol.* 25, 134–140 (1986).

Case 2 from Satoru Kudose, MD, Columbia University Irving Medical Center

A 42-year-old woman with thyroid nodule, anxiety, anemia, and suspected glaucoma presented with proteinuria. The patient had no history of tobacco use. Family history was significant for an 85-year-old father with kidney failure at age 70 who underwent renal transplantation. Other relatives reportedly did not have kidney disease. Physical exam showed blood pressure 130/74 mmHg, BMI 29.3 kg/m^2, and no lower extremity edema. The patient's medications included sertraline and valsartan. Laboratory evaluation revealed serum creatinine 0.64 mg/dl, 24-hour urine protein 2.5 g, and serum albumin 3.8 g/dl. Serologic evaluation, including serum C3, C4, anti-phospholipase A2 receptor antibodies, and hepatitis panel, was unremarkable. Serum protein electrophoresis with immunofixation did not reveal paraprotein.

Light Microscopy:
A glomerulus (H&E, left, and PAS, right):

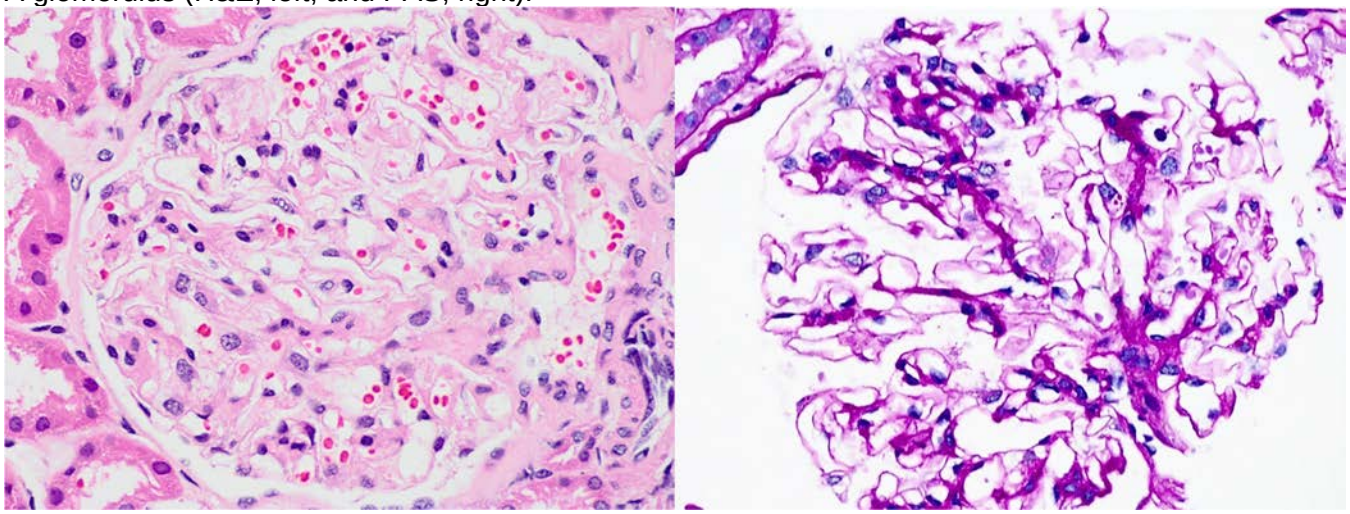

A glomerulus (JMS, left, and toluidine blue, right):

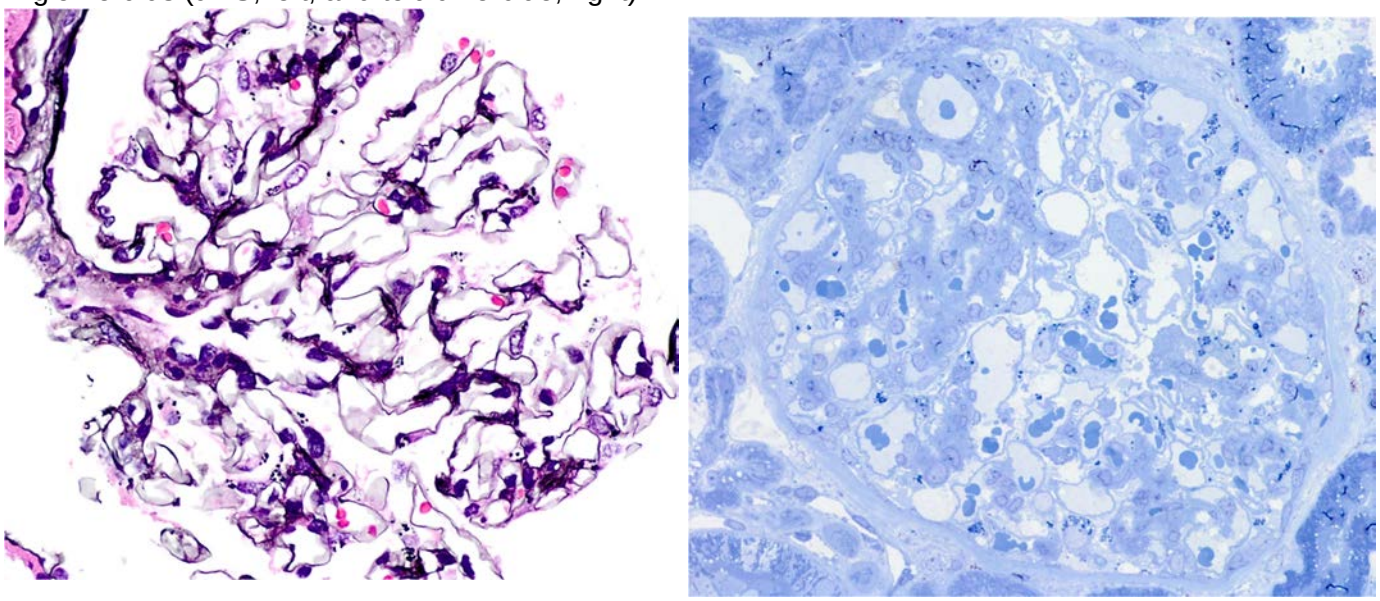

Interstitial foam cells (left, H&E) and tubulointerstitial scarring (right, PAS):

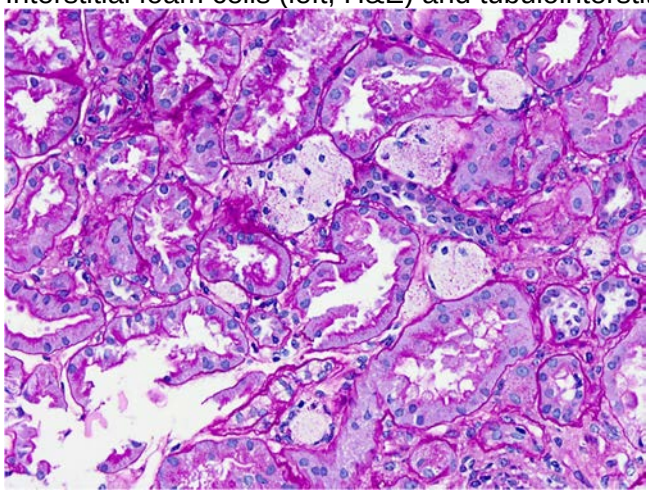

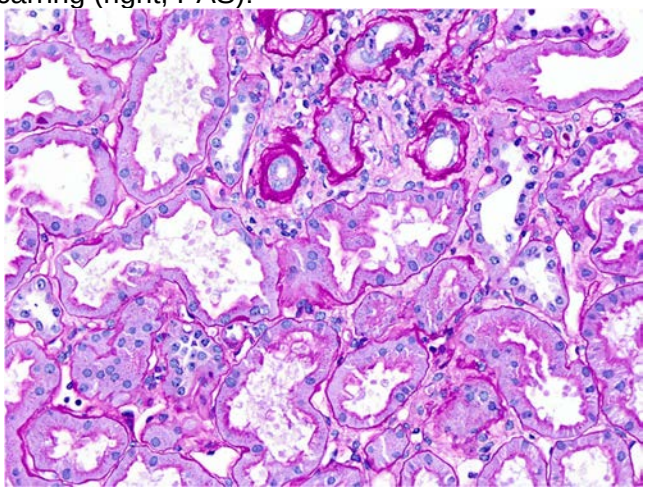

Immunofluorescence Microscopy: Noncontributory.

Electron Microscopy:
Myelin figures:

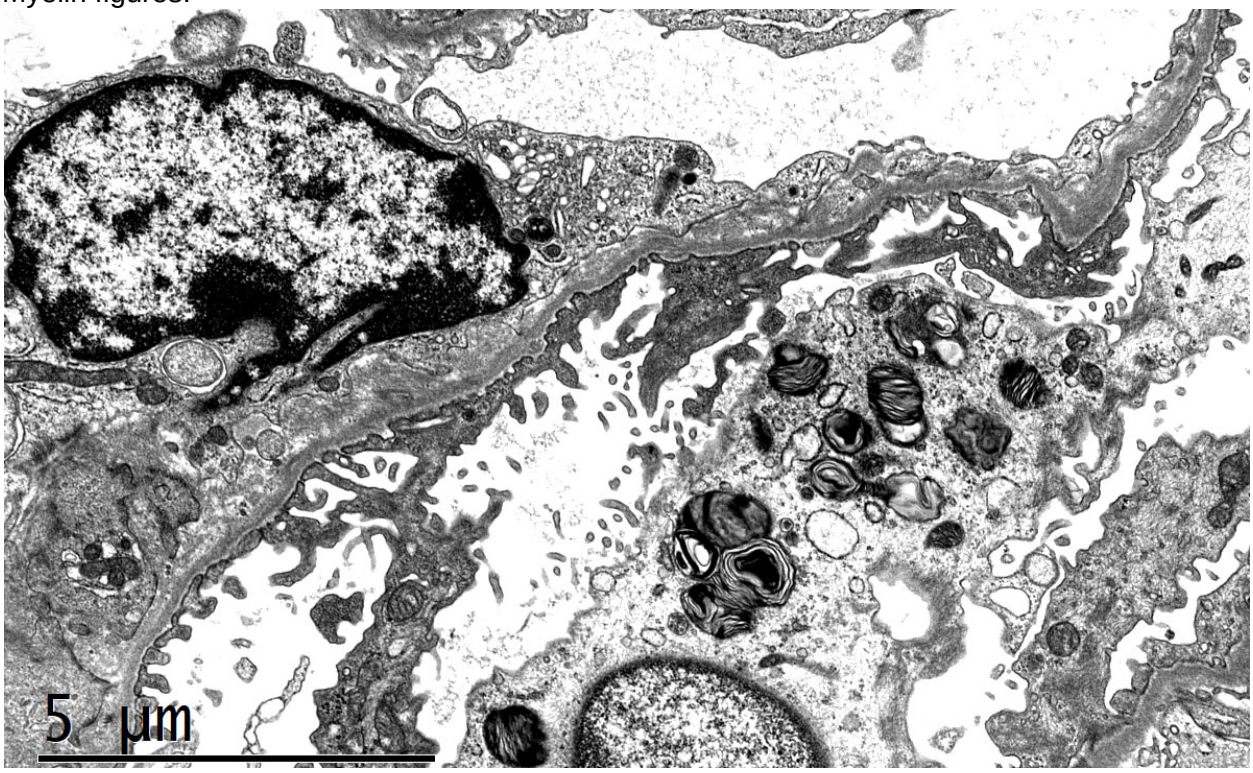

Distinct bundles of curvilinear fibrils:

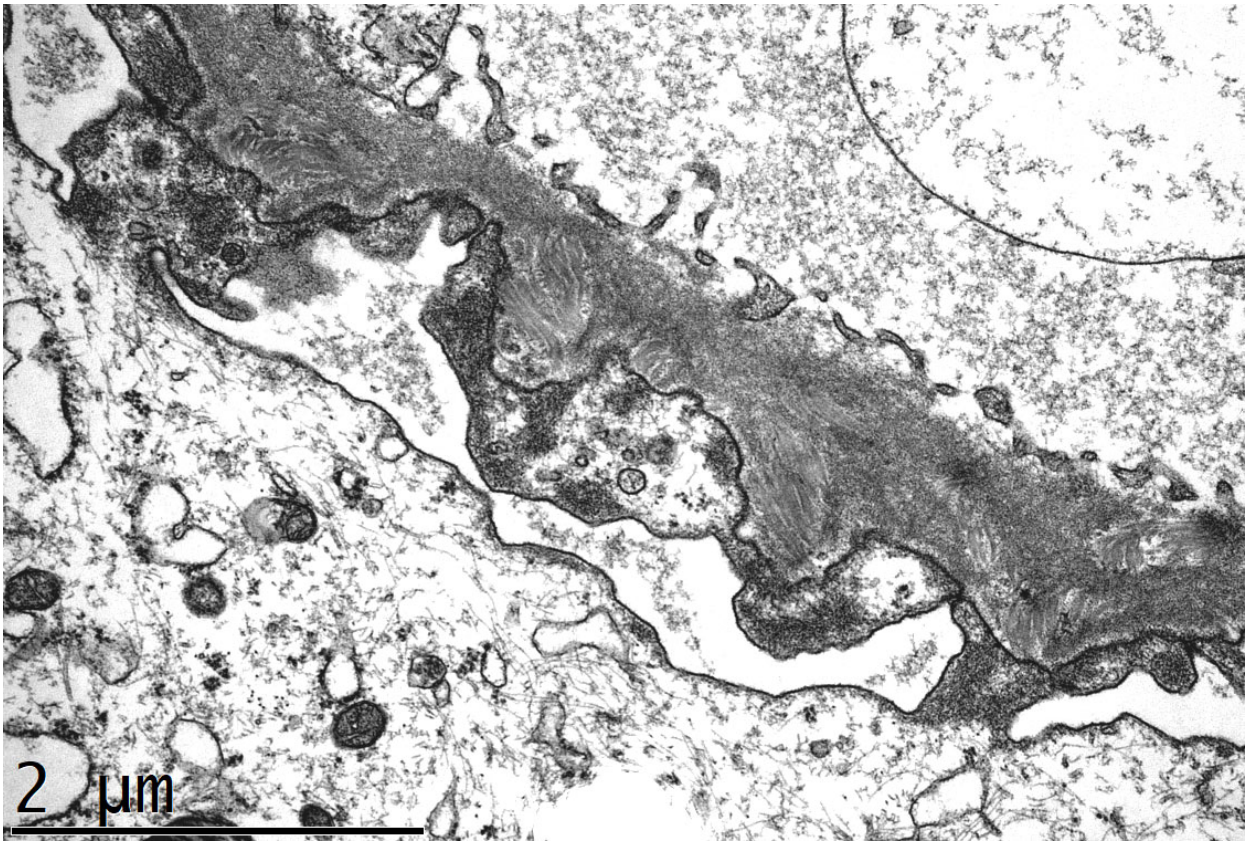

Distinct bundles of curvilinear fibrils (higher magnification):

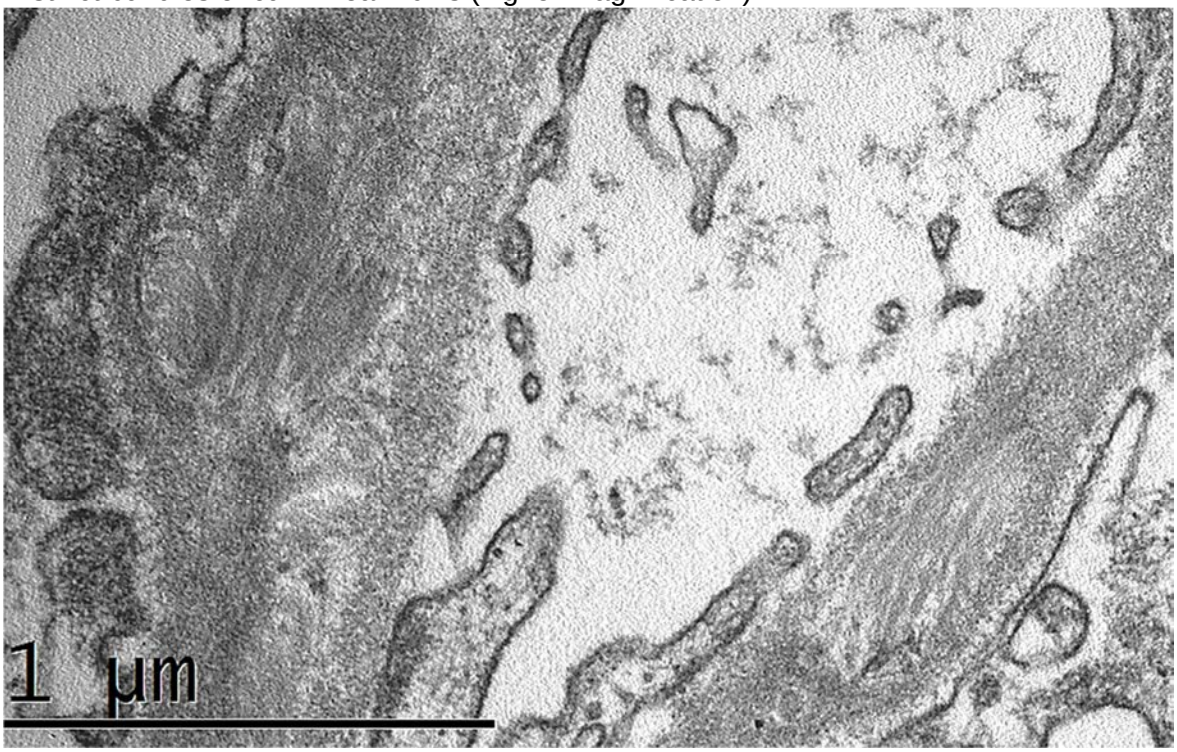

Areas with more subtle involvement:

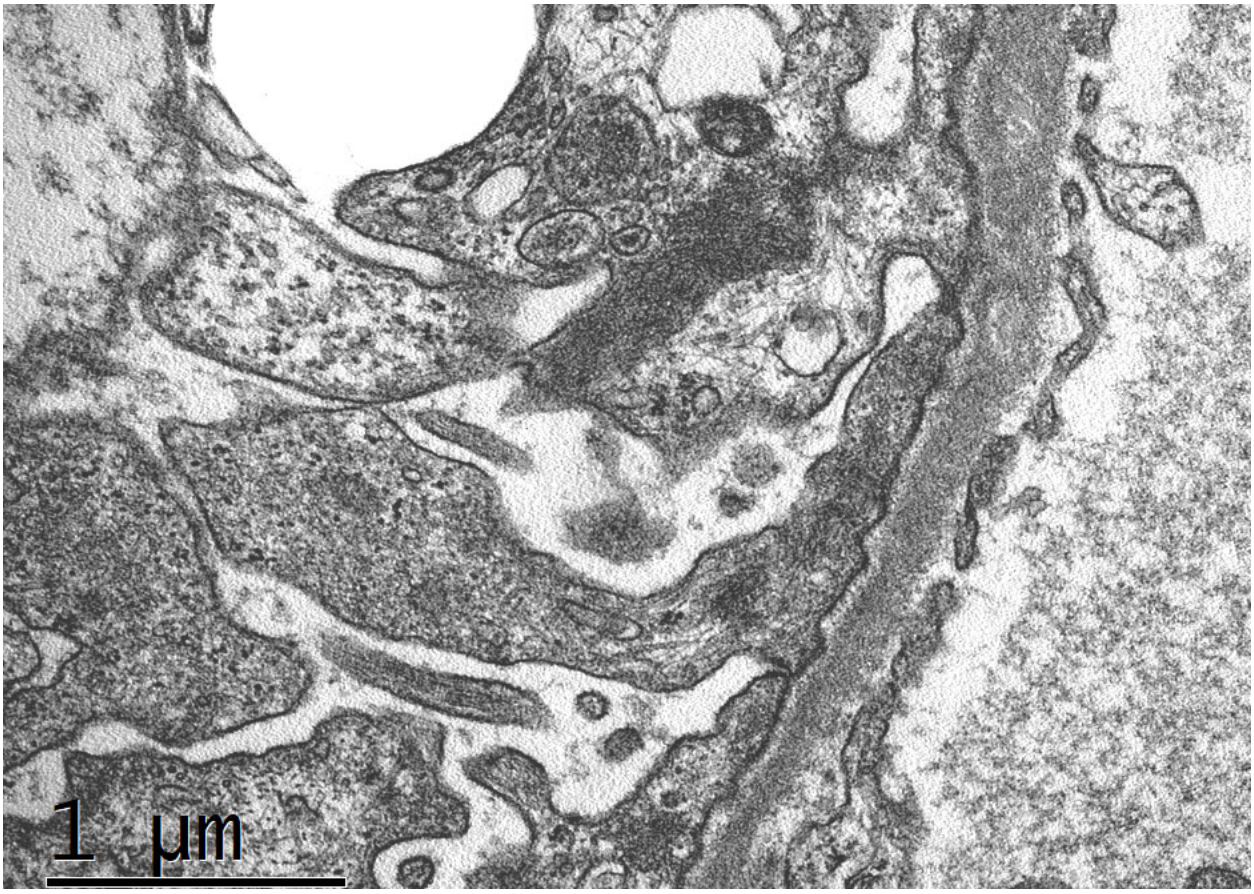

Pathologic Findings

Light Microscopy: Sampling for light microscopy demonstrated five cores of renal cortex, including two with medulla, and one core of medulla only. Of 15 glomeruli, one was globally sclerotic. The remaining glomeruli ranged from normal in size to mildly enlarged and demonstrated normal cellularity with largely patent capillary lumina. The glomerular basement membranes (GBMs) appeared normal in thickness without duplication. Proximal tubules appeared unremarkable. Scattered interstitial foam cells were present. There was ~20% tubulointerstitial scarring, accompanied by sparse inflammatory infiltrates confined within the scarred areas. No significant tubulitis was seen. Vessels were unremarkable.

Immunofluorescence Microscopy: Routine immunofluorescence demonstrated trace staining for IgM in the mesangial distribution (scale 0, trace, 1-3+). There was no significant glomerular staining for other reactants.

Electron Microscopy: Ultrastructural examination demonstrated glomeruli with unremarkable mesangium. The GBMs were predominantly normal in thickness and texture. However, there were occasional areas with textural irregularity and electron lucent areas. Examination at higher magnification revealed that some of these areas demonstrate predominantly intramembranous bundle of fibrillar material with appearance consistent with collagen. In addition, podocytes diffusely demonstrated intracytoplasmic myelin figures. There were no electron dense deposits or endothelial tubuloreticular inclusions.

Diagnosis

Nail-patella syndrome/LMX1B related nephropathy and, possibly, renal phospholipidosis such as related to sertraline use

Clinical Follow-Up

The patient underwent genetic testing (Natera Renasight™) and was found to have a pathogenic mutation in *LMX1B* [c.746G>A (p.Arg249Gln)]. There was no mutation in *COL4A3, 4 or 5*, or in *GLA* (typical of Alport syndrome and Fabry disease, respectively). Due to this finding, her physical exam was reviewed. She had no muskuloskeltal features of nail-patella syndrome. In addition, her father was also tested and was found to have the same mutation.

Questions for Case 2

1. Kidney biopsy demonstrates podocytes containing myelin figures (also known as zebra bodies).

Which of the following is/are a possible etiology for this finding? (select all that apply)

A. Medication-induced phospholipidosis
B. Fabry disease
C. Nail-patella syndrome
D. Diabetic nephropathy

Podocytes with myelin figures can be seen in the setting of Fabry disease, medication-induced phospholipidosis, and in nail-patella syndrome.

2. Kidney biopsy demonstrates podocytes containing myelin figures (also known as zebra bodies). The patient undergoes genetic testing and there is no mutation of *GLA* or *LMX1B* (genes associated with Fabry disease and nail-patella syndrome, respectively).

Which of the following medications could be responsible for this finding?

A. Hydroxychloroquine
B. Lisinopril
C. Valproic acid
D. Gentamicin

There are reports of myelin figures in podocytes in patients taking hydroxychloroquine. In patients with gentamicin use, myelin figures are usually in tubular epithelial cells. Lisinopril and valproic acid have not been reported to be associated with iatrogenic renal phospholipidosis.

3. Which of the following is the ultrastructural finding characteristic of nail-patella syndrome?

A. Collagen bundle within the GBMs
B. Collagen bundle within the hilar areas only
C. Collagen bundle within the mesangium and subendothelial areas
D. Randomly oriented fibrils in the mesangium and in the GBMs, measuring ~8 nm

Collagen bundles within the GBMs are characteristic of nail-patella syndrome. Hilar areas of the glomeruli normally contain collagen bundles. This is called a "central fibrous area" in the literature and is thought to be more common in older patients. Collagen bundles in the mesangial and subendothelial areas can be seen in type III collagen glomerulopathy and in familial nephropathy and multiple exostoses with EXT1 mutation. Randomly oriented ~8 nm fibrils are characteristic of amyloidosis.

Discussion

Most common etiologic considerations for myelin figures in podocytes include Fabry disease and drug-induced/iatrogenic phospholipidosis. Fabry disease is caused by mutations in α-galactosidase A on chromosome X, resulting in accumulation of sphingolipids in various tissues, including mesangial, endothelial cells, and tubular epithelial cells in the kidneys. Drug-induced phospholipidosis is caused by cationic amphiphilic medications that contain hydrophilic and hydrophobic regions, which bind and make phospholipids resistant to phospholipases. The most well-known such medications include chloroquine, hydroxychloroquine, and amiodarone, though over 50 medications have been reported, including sertraline and hydralazine according to a recent report.[1] In the kidneys, podocytes are the most frequent cells to contain myelin figures, though this differs depending on the culprit medication (for example, tubular epithelial cells in patients with gentamicin use). Of note, though likely related to the severity of involvement, clinical correlation is necessary to determine the renal significance of myelin figures.

Nail-patella syndrome is caused by a mutation in *LMX1B*, characterized by abnormalities in nail and patella, with autosomal dominant pattern of inheritance.[2] However, proteinuric CKD and ocular involvement can also be present, similar to Alport syndrome and Fabry disease. Light microscopic findings in nail-patella syndrome, Alport syndrome, and Fabry disease can also be alike, with light microscopy demonstrating focal segmental and/or global glomerulosclerosis with glomerulomegaly, with or without interstitial foam cells, depending on the chronicity of proteinuria.[3] These entities can be distinguished by their ultrastructural features. The characteristic features of Alport syndrome are the glomerular basement thinning or textural abnormality and that of Fabry disease are myelin figures in podocytes and other cells. The characteristic features of nail-patella syndrome are the GBM textural abnormality and intramembranous bundle of fibrils, consistent with type III collagen, best seen when the sample for electron microscopy is stained with phosphotungstic acid, a stain not routinely used in practice.

However, a few cases of podocytes with myelin figures have been recently reported in patients with *LMX1B*-associated nephropathy.[3-5] In these reports, myelin figures were predominantly in podocytes, though also rarely present in other cell types. These patients had mutations in the homeodomain of *LMX1B* (p.Arg246Gln in two families and one patient, and p.Arg249Gln in one patient), a site of mutation that typically lacks extrarenal features of nail-patella syndrome.[2, 6] No patient had exposure to medications known to be associated with myelin figures, though the medication list is not available for independent review. Regardless, the presence of myelin figures in multiple family members in one report suggests that myelin figures may be due to a *LMX1B* mutation itself,[3] though the mechanism for the formation of myelin figures is not known.

This case underscores the need to consider nail-patella syndrome/*LMX1B*-associated nephropathy together with Fabry disease in patients with myelin bodies in their kidney biopsies. This is because (1) extrarenal features can be subtle or absent in both nail-patella syndrome/*LMX1B*-associated nephropathy and in Fabry disease, especially in female heterozygous patients, and (2) the characteristic ultrastructural features of nail-patella syndrome can be rare and are not optimally visualized using routinely used staining procedures.

Furthermore, given the rarity of the reports of myelin figures in *LMX1B*-associated nephropathy, the possibility of medication-induced phospholipidosis should also be considered.

References

1. Choung HYG, Jean-Gilles J, Goldman B. Myeloid bodies is not an uncommon ultrastructural finding. *Ultrastruct Pathol* 2022; 46: 130-138.
2. Harita Y, Kitanaka S, Isojima T, et al. Spectrum of LMX1B mutations: from nail-patella syndrome to isolated nephropathy. *Pediatr Nephrol* 2017; 32: 1845-1850.
3. Lei L, Oh G, Sutherland S, et al. Myelin bodies in LMX1B-associated nephropathy: potential for misdiagnosis. *Pediatr Nephrol* 2020; 35: 1647-1657.
4. Pinto EVF, Pichurin PN, Fervenza FC, et al. Nail-patella-like renal disease masquerading as Fabry disease on kidney biopsy: a case report. *BMC Nephrol* 2020; 21: 341.
5. Shimohata H, Miyake Y, Yoshida Y, et al. LMX1B-associated nephropathy that showed myelin figures on electron microscopy. *CEN Case Rep* 2021; 10: 588-591.
6. Boyer O, Woerner S, Yang F, et al. LMX1B mutations cause hereditary FSGS without extrarenal involvement. *J Am Soc Nephrol* 2013; 24: 1216-1222.

Case 3 from Laura Finn, MD, Children's Hospital of Philadelphia, University of Pennsylvania

A 6-year-old girl, born at term with a normal infancy, had no significant past medical history except for eczema and sensitive skin. No medications or allergies were reported. The family history was only significant for renal calculi in father and maternal uncle. Two months prior to presentation, the patient was diagnosed with flu and had a negative strep culture. Height and weight were in the 90th and 50th percentile, respectively. Physical exam was appropriate and unremarkable; specifically, the patient lacked periorbital and pedal edema, palpable kidneys, rash, and arthritis. Urine had 3+ protein, microscopic hematuria, and specific gravity of 1.030. Relevant laboratory results included: normal renal function, serum albumin, cholesterol, C3 and C4 levels; and negative ANA and ASO titers. Urine protein excretion was 2 gm/24 hours.

Light Microscopy:

Fig 1. Trichrome:

Fig 2. PAS:

Fig 3. PAS:

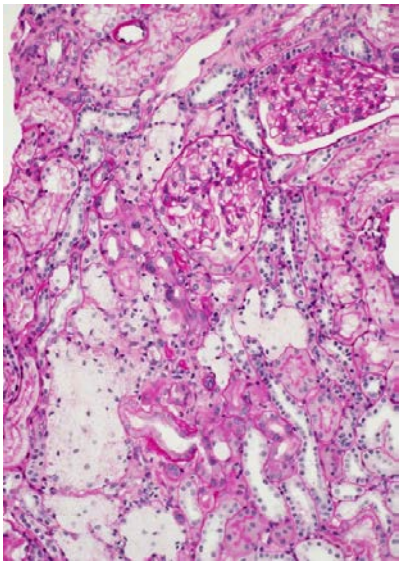

Fig 4. Jones:

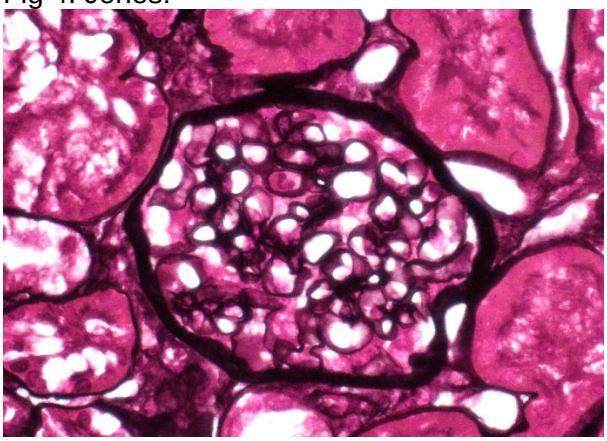

Fig 5. H&E:

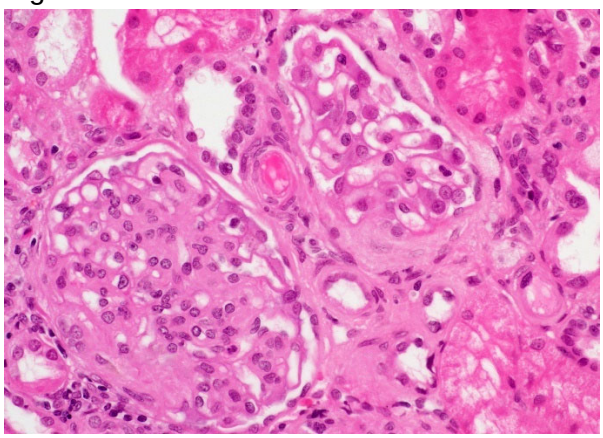

Fig 6. Immunofluorescence Microscopy (IF) (IgM):

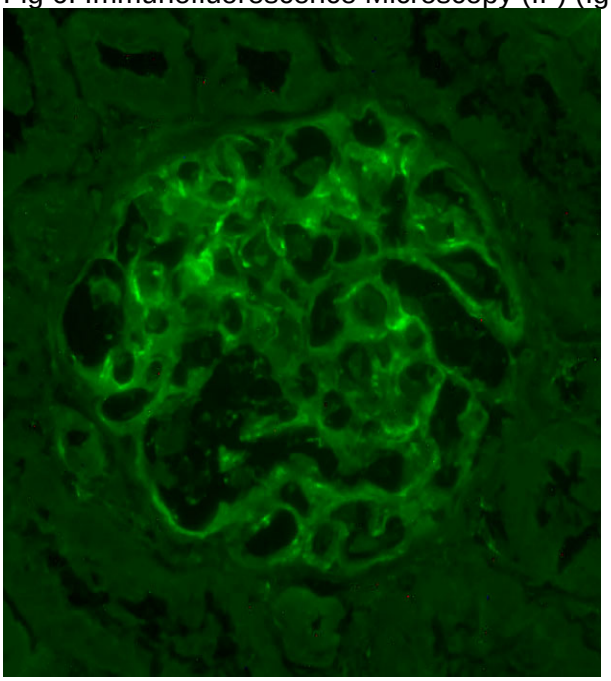

Fig 7. Electron Microscopy (EM):

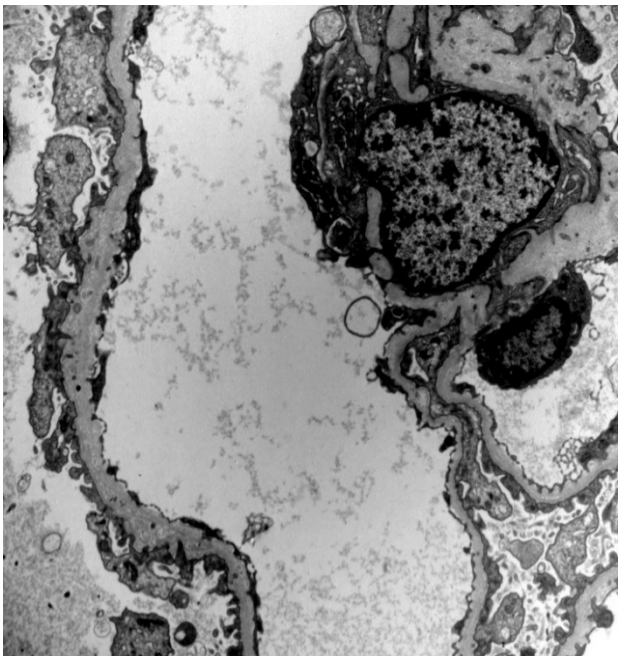

Fig 8. EM:

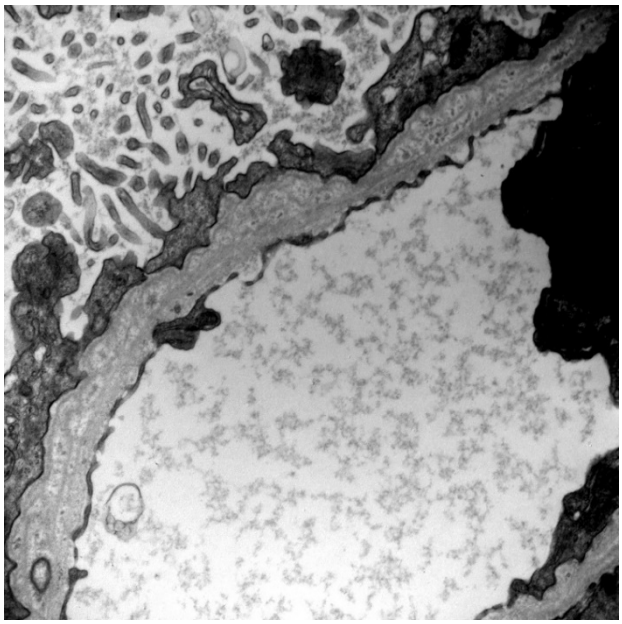

Pathologic Findings

Light Microscopy: The kidney biopsy consisted of two cores, one containing only medulla and the other, cortex with 10–12 glomeruli/level. Trichrome stain highlighted patchy interstitial fibrosis and tubular atrophy that occupied 10–15% of the cortex (Figure 1). Two glomeruli were globally sclerotic (Figure 2). A subset had mild segmental mesangial expansion with hypercellularity (Figure 3), but the majority were normal (Figure 4). A single glomerulus had features of segmental sclerosis, and rare glomeruli had periglomerular fibrosis (Figures 5). The interstitium contained occasional clusters of foam cells (Figures 1 and 3).

Immunofluorescent Microscopy: Routine immunofluorescence staining on frozen tissue showed trace to 1+ nonspecific mesangial IgM (Figure 6). Other immunoreactants were negative.

Electron Microscopy: There was extensive foot process effacement associated with microvillous transformation. Nearly all of the glomerular capillary basement membranes were abnormal, showing varying degrees of expansion (up to 750 nm) with few thin segments (< 200 nm) (Figure 7). Irregular areas had mottling and multilamellation throughout the lamina densa as well as scalloping of the subepithelial and subendothelial glomerular basement membrane (GBM) (Figure 8). The membranes contained occasional dense structures suggestive of lipid. No immune complexes were identified.

Initial Diagnostic Interpretation

Features consistent with Alport syndrome and associated segmental and global glomerulosclerosis

Clinical Follow-Up

The patient was maintained on ACE inhibition with stable renal function. Investigation of delayed puberty and primary amenorrhea at 15 years of age led to a diagnosis of hypergonadotropic hypogonadism, and she was started on hormone therapy. Concurrent testing revealed a normal XY karyotype. Over the next few years, her renal function declined, and she was listed for transplantation. At age 18, metastatic dysgerminoma was diagnosed from a cervical lymph node biopsy. Molecular analysis disclosed a germline heterozygous *WT1* intronic variant (c.1447+5G>A) considered pathogenic for Frasier syndrome. After chemotherapy, she underwent bilateral nephrectomies and removal of bilateral adnexa, which showed bilateral fallopian tubes, streak gonad (right), and necrotic tumor arising in a streak gonad (left). Both kidneys had end-stage alterations of diffuse global glomerulosclerosis and tubulointerstitial fibrosis with inflammation. She received a kidney transplant at age 21 (2023) and remains tumor free.

Final Diagnosis

Segmental and global glomerulosclerosis secondary to WT1 intron 9 variant (Frasier syndrome)

Questions for Case 3

1. **What is the glomerular pattern depicted in Fig 4 (Jones)?**

    A. Membranous
    B. Membranoproliferative
    C. Mesangioproliferative
    D. Normal

    The Jones methenamine silver stain demonstrates open capillary loops surrounded by uniform GBMs devoid of spikes or holes (membranous), or duplication (membranoproliferative). The mesangial nuclei number 3 or fewer per glomerular segment (≥4 considered hypercellular). A normal glomerulus by light microscopy does not preclude finding immune complexes (IF; example, IgA nephropathy) or ultrastructural basement membrane or podocyte abnormalities (EM; example Alport syndrome and minimal change disease).

2. **Interstitial foam cells in a kidney biopsy are most suggestive of which condition?**

    A. Proteinuria
    B. Hematuria
    C. Infection
    D. Metabolic/storage disease

    Interstitial foamy macrophages containing lipid and lipoproteins (foam cells) in a kidney biopsy are most commonly associated with nephrotic syndrome, prolonged proteinuria, or hyperlipidemia. Notably, they are a frequent finding in Alport syndrome, even with non-nephrotic proteinuria, but are infrequently reported in IgA nephropathy. Glomerular foam cells are often seen with FSGS (tip lesion and cellular variant) and diabetic nephropathy. Kidney infections typically contain neutrophilic or lymphoplasmacytic infiltrates, rather than foam cells; occasionally, granulomatous inflammation is found with certain organisms. So-called xanthogranulomatous pyelonephritis is characterized by a fibroinflammatory rind surrounding sheets of foamy macrophages, in association with extensive parenchymal injury. This infrequent condition is usually not biopsied. Interstitial foam cells are occasionally found in rare metabolic diseases such as familial lecithin-cholesterol acyltransferase deficiency, Fabry disease, and uncommonly in lipoprotein glomerulopathy, but are accompanied by unique glomerular lesions.

3. **Abnormalities in glomerular basement membranes may be seen by electron microscopy in which disorder? (select all that apply)**

    A. Pediatric donor glomerulopathy
    B. Alport syndrome
    C. IgA nephropathy
    D. Frasier syndrome

    Laminated GBM with a "basket-weave" appearance is a classic finding in Alport syndrome and its variants, where it may also be associated with GBM thinning. Not uncommonly, GBM lamellations are also seen in glomerulopathy associated with WT1 mutations (Frasier and Denys-Drash syndromes) and LAMB2 mutations (Pierson syndrome). Thickened and irregular ("moth-eaten") glomerular capillary walls are also

found in nail-patella syndrome (LMX1B mutation). Non-syndromic causes of GBM irregularities that might mimic Alport or Frasier syndromes include IgA nephropathy, pediatric donor (size-mismatch) glomerulopathy due to stress adaptation, resolving immune complex-mediated glomerulonephritides, and chronic endothelial cell injury, such as chronic thrombotic microangiopathy or transplant glomerulopathy.

Discussion

Defects in the alpha 3, alpha 4, and alpha 5 chains of type 4 collagen are responsible for Alport syndrome, which classically presents with hematuria that manifests as GBM thinning and lamellation[1]. Inheritance patterns including X-linked, autosomal recessive, autosomal dominant, and digenic reflect gene variants which significantly influence the clinical progression and the presence of extrarenal manifestations[2]. The kidney biopsy may initially appear normal by light microscopy and often contains clusters of foam cells in the interstitium. Glomerular and interstitial fibrosis ensue as the disease progresses. Historically, the diagnosis was made by finding characteristic GBM alterations visible by electron microscopy. Immunofluorescent staining for the alpha 5 chain can be useful when an aberrant pattern is demonstrated. Were the biopsy on this patient performed today, rather than in 2008, the molecular testing for pathogenic variants in *COL4A3-COL4A5* would undoubtedly have been performed in accord with current guidelines[3].

Although characteristic, electron microscopic GBM alterations are not pathognomonic of *COL4*-related nephropathy, but resemble those found in *WT1*-, *ITGA3/B4*- and *LAMB2*-related nephropathies, and show overlap with the EM findings sometimes seen in various nonsyndromic disorders such as IgA nephropathy, chronic endothelial injury, glomerular hypertension, and hyperfiltration, and even resolving immune-complex disease.

As this patient aged, a clinical phenotype (and genotype) including delayed puberty, XY karyotype, streak gonads, malignant transformation of presumed gonadoblastoma to dysgerminoma, and pathogenic germline *WT1* intron 9 splicing donor site variant were unveiled, supporting a diagnosis of Frasier syndrome[4,5], rather than Alport syndrome.

The *WT1* gene plays an essential role in urogenital and kidney development. With the advance of genetic tools, it is becoming apparent that *WT1*-related disorders comprise a wide phenotypic spectrum beyond the classic syndromes of Denys-Drash (DDS; congenital nephrotic syndrome with diffuse mesangial sclerosis, 46 XY disorder of sexual development with sex reversal (DSD) and Wilms tumor), Frasier (FS; FSGS, 46XY DSD, and gonadoblastoma), Meacham (congenital diaphragmatic hernia, cardiac malformations and genitourinary malformations) and WAGR (Wilms tumor, aniridia, genitourinary malformations and variable mental retardation). Despite an observed genotypic-phenotypic correlation, ≤25% of those with exon 8–9 missense mutations and <75% of those with KTS intron 9 variants have the classic syndromic phenotype of DDS and FS, respectively[6,7].

Mutations in the *WT1* splice donor sites within intron 9 create an imbalance in the two crucial transcripts, altering the usual constant ratio of +KTS/-KTS isoforms from approximately 1.5 to 0.5. The resulting disequilibrium causes gonadal abnormalities because *WT1* is critical for the differentiation and maintenance of Sertoli cells through its activation of *SRY* (located on the Y chromosome); the +KTS isoform appears to be more efficient at this activation. Sertoli cells in the male fetus produce mullerian inhibiting factor (MIF), the absence of which can result in sex reversal[8]. In addition, an increase in the -KTS isoform appears to accelerate granulosa cell (ovarian stromal cells that produce estrogen and progesterone) differentiation, which also contributes to phenotype.

In the fetal kidney, *WT1* is expressed in areas of active glomerulogenesis, and expression persists in the podocyte after completion of nephrogenesis, thus supporting a role in the development, maturation, and maintenance of the glomerular filtration barrier. Recent analyses have shown that *WT1* binds to promoters and enhancers of about half of the known 200 podocyte-specific genes (including *NPHS1* and *NPHS2*), and in mice lacking +KTS isoforms, there is down regulation of some of these genes. In addition to the slit-diaphragm, *WT1* controls focal adhesion via regulation of integrins (α3 and β1) and laminins (α5 and β2), and cytoskeletal maintenance (i.e., *ACTN4, MYH9,* and *ARHGAP24*) that together establish podocyte polarity[9,10].

Persistent and progressive proteinuria is the most common finding in *WT1* glomerulopathy. Recent cohort series suggest that *WT1* mutations account for ~5–15% of steroid-resistant nephrotic syndrome (SRNS) and 28–33% of congenital nephrotic syndrome. In individuals with isolated SRNS, *WT1* is among the top three most commonly mutated genes, accounting for approximately 5% of cases[11,12], although monogenic causes may vary among different populations. Nearly all patients with isolated *WT1*-associated SRNS are genotypic and phenotypic females[13].

References

1. Hudson BG, Tryggvason K, Sundaramoorthy M, et al. Alport's syndrome, Goodpasture's syndrome, and type IV collagen. *N Engl J Med* 2003; 348:2543-56.
2. Kashtan CE, Ding J, Garosi G, et al. Alport syndrome: a unified classification of genetic disorders of collagen IV alpha345: a position paper of the Alport Syndrome Classification Working Group. *Kidney Int* 2018; 93:1045-1051.
3. Savige J, Lipska-Zietkiewicz BS, Watson E, et al. Guidelines for Genetic Testing and Management of Alport Syndrome. *Clin J Am Soc Nephrol* 2022; 17:143-154.
4. Barbaux S, Niaudet P, Gubler MC, et al. Donor splice-site mutations in WT1 are responsible for Frasier syndrome. *Nat Genet* 1997; 17:467-70.
5. Klamt B, Koziell A, Poulat F, et al. Frasier syndrome is caused by defective alternative splicing of WT1 leading to an altered ratio of WT1 +/-KTS splice isoforms. *Hum Mol Genet* 1998; 7:709-14.
6. Lipska BS, Ranchin B, Iatropoulos P, et al. Genotype-phenotype associations in WT1 glomerulopathy. *Kidney Int* 2014; 85:1169-78.
7. Lopez-Gonzalez M, Ariceta G. WT1-related disorders: more than Denys-Drash syndrome. *Pediatr Nephrol* 2024; 39:2601-2609.
8. Hastie ND. Wilms' tumour 1 (WT1) in development, homeostasis and disease. *Development* 2017; 144:2862-2872.
9. Dong L, Pietsch S, Englert C. Towards an understanding of kidney diseases associated with WT1 mutations. *Kidney Int* 2015; 88:684-90.
10. Lefebvre J, Clarkson M, Massa F, et al. Alternatively spliced isoforms of WT1 control podocyte-specific gene expression. *Kidney Int* 2015; 88:321-31.
11. Sadowski CE, Lovric S, Ashraf S, et al. A single-gene cause in 29.5% of cases of steroid-resistant nephrotic syndrome. *J Am Soc Nephrol* 2015; 26:1279-89.
12. Trautmann A, Bodria M, Ozaltin F, et al. Spectrum of steroid-resistant and congenital nephrotic syndrome in children: the PodoNet registry cohort. *Clin J Am Soc Nephrol* 2015; 10:592-600.
13. Trautmann A, Lipska-Zietkiewicz BS, Schaefer F. Exploring the clinical and genetic spectrum of steroid resistant nephrotic syndrome: The PodoNetRegistry. *Front Pediatr* 2018;6:200.

Case 4 from Ritu Gupta, MD, Mount Sinai Medical Center, Mount Sinai Hospital

A 35-year-old woman with history of hypertension (on labetalol) and fibroids and no significant family history with proteinuria found on dipstick (>300mg/dL urine protein) during pre-operative workup for laparoscopic myomectomy was lost to follow-up. She presented to outpatient nephrology eight months later for follow-up of proteinuria, was found to have UPCR 5g and microhematuria, and was noted to be 10 weeks pregnant. Serologic testing was negative, including ANA, ANCA, hepatitis B and C, HIV, anti-PLA2R, RF, anti-dsDNA, anti-Smith, anti-CCP, anti-chromatin, and cryoglobulins. Other labs showed C3 107, C4 36, serum creatinine 0.8, and no paraprotein. The patient was ultimately scheduled for a biopsy about 1 month later. At the time of biopsy, labs showed serum creatinine 1.4, hematuria, and 10g proteinuria.

Light Microscopy:
Fig 1

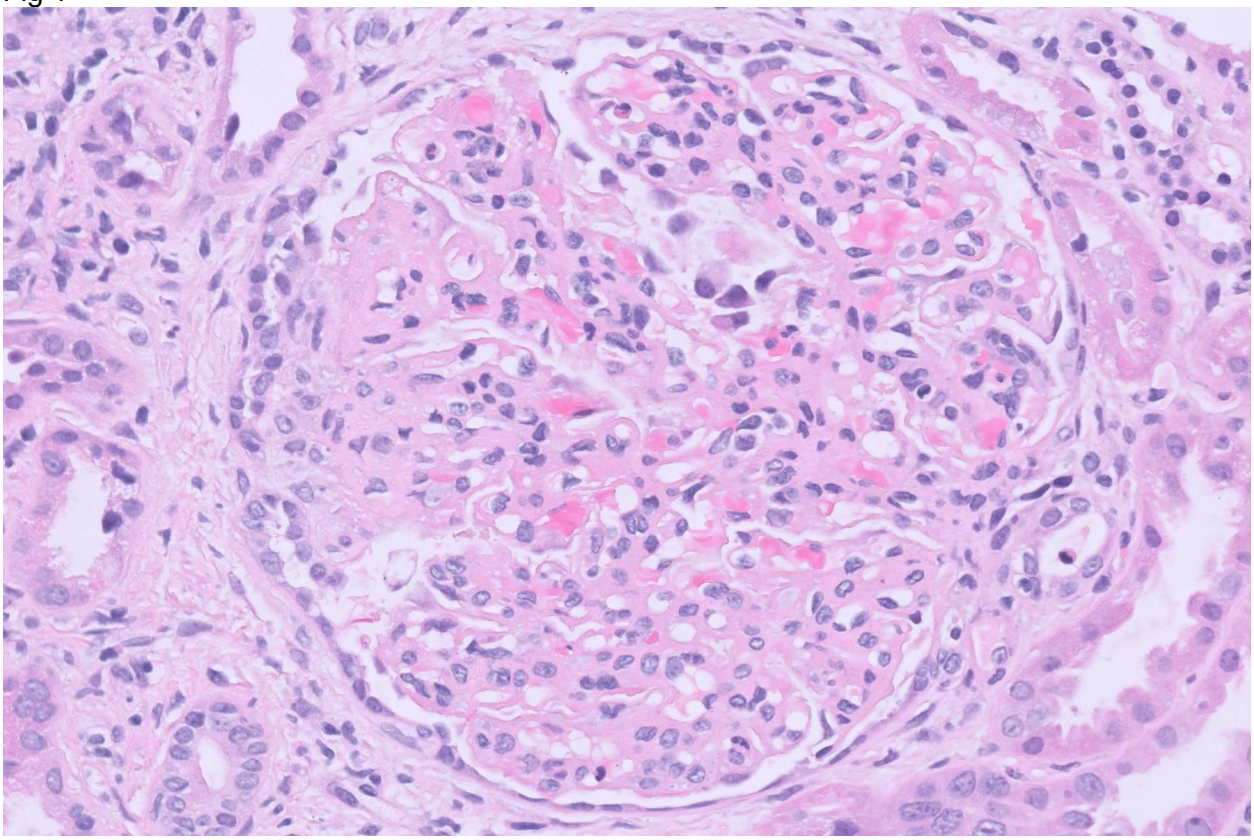

Fig 2

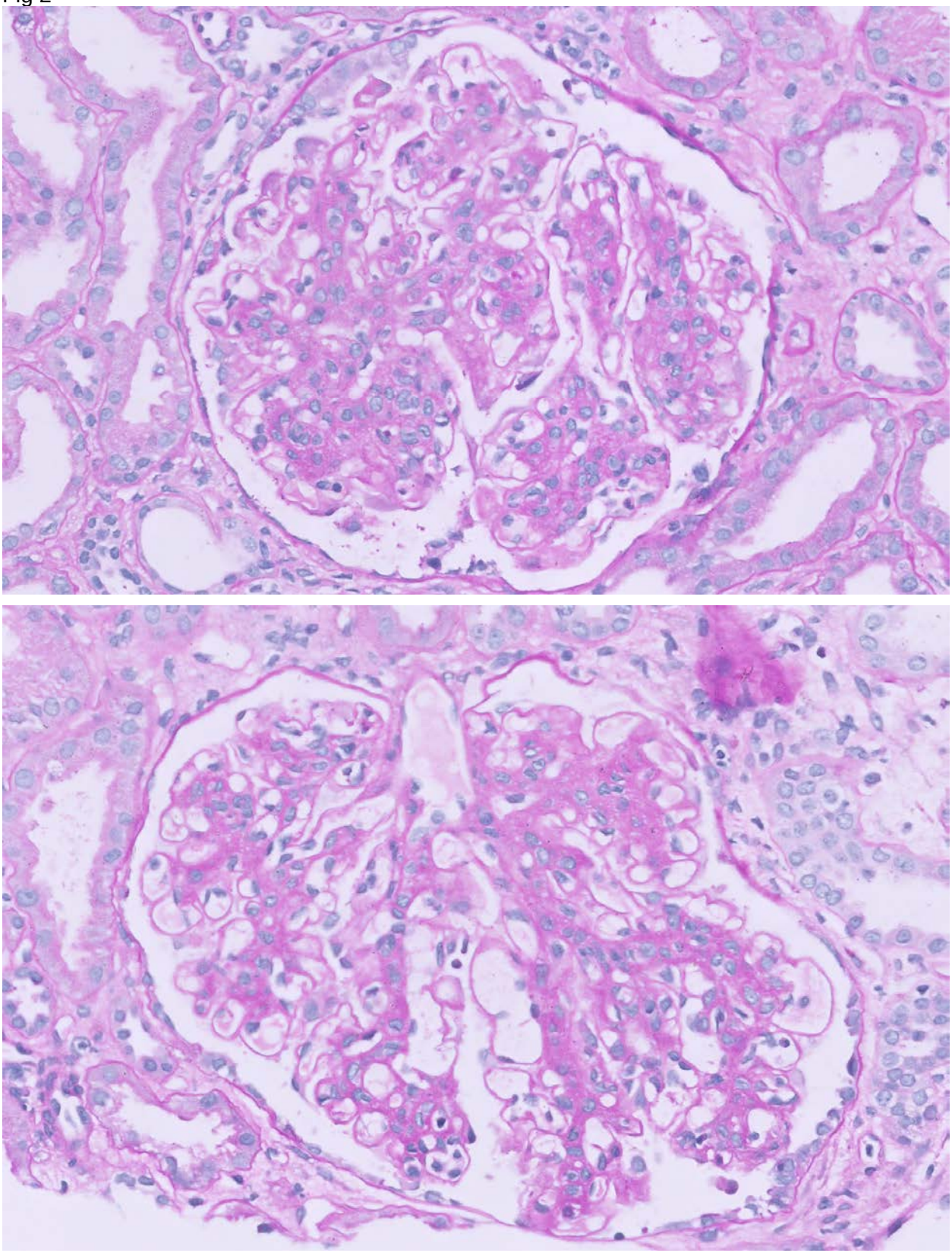

Fig 3

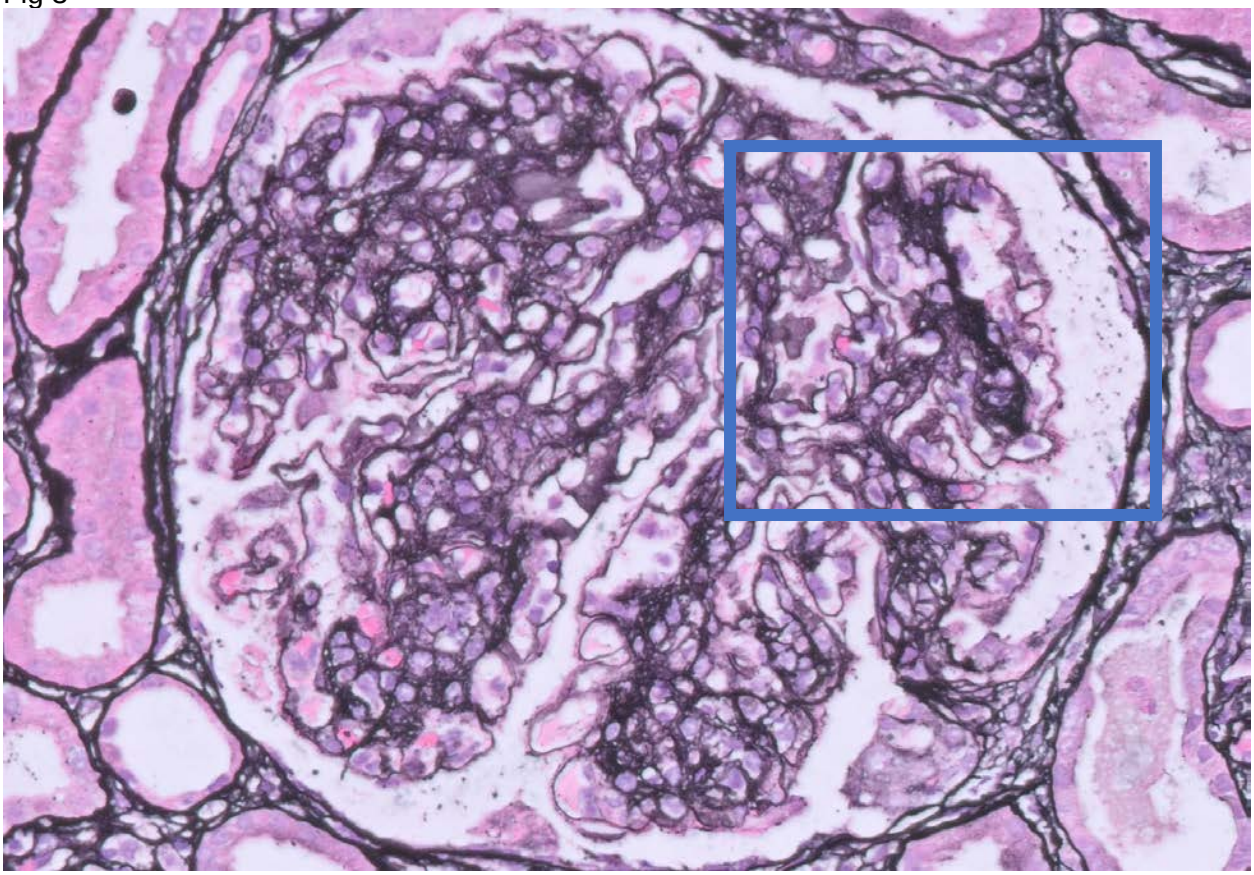

Insert:

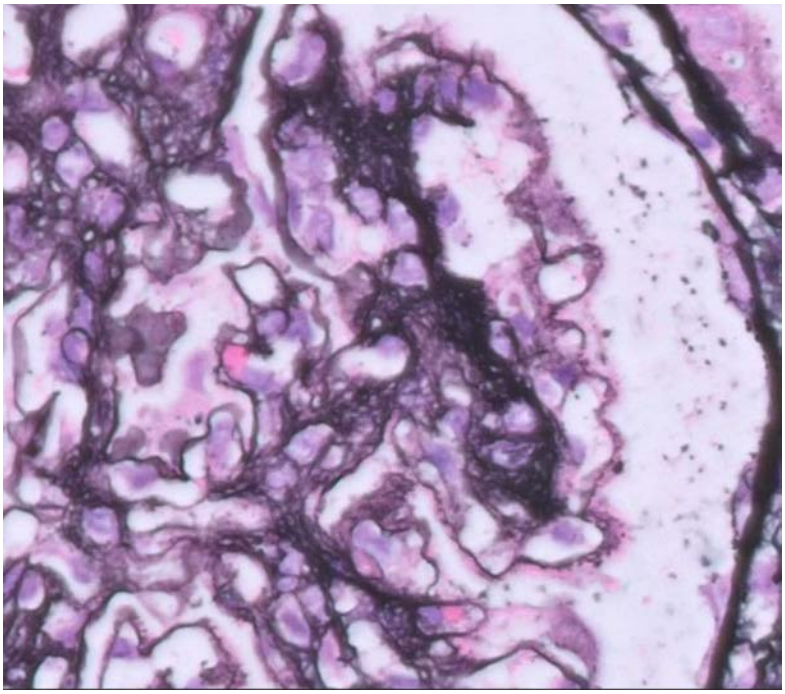

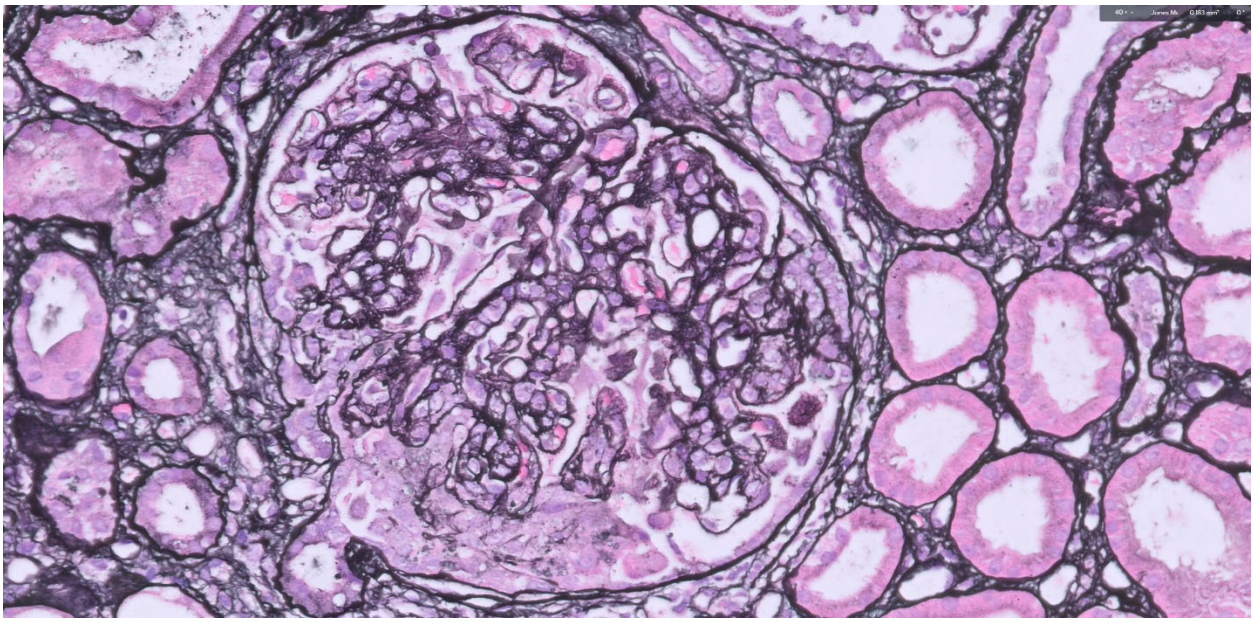

Fig 4: Immunofluorescence Microscopy (IF) (IgG)

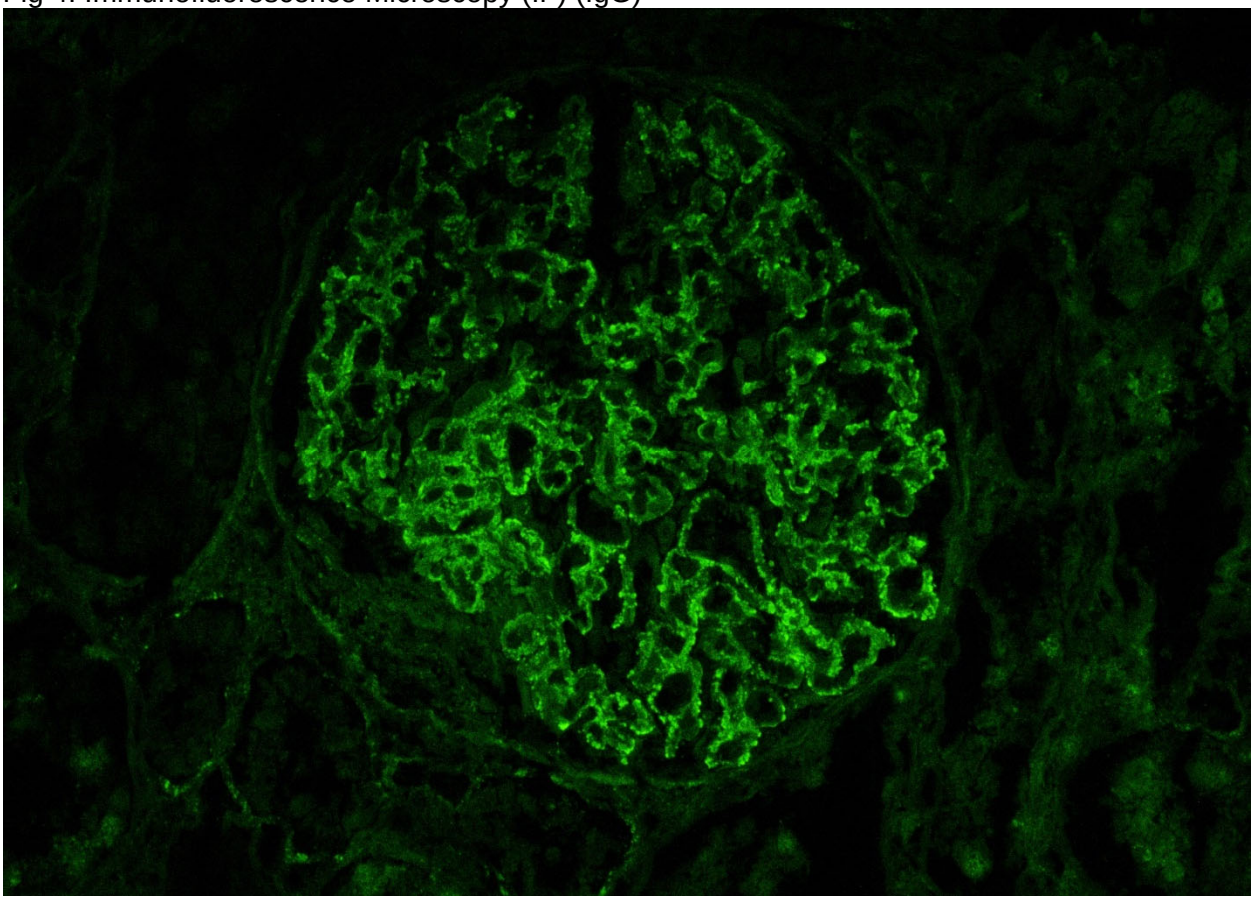

Fig 4: IF (IgA)

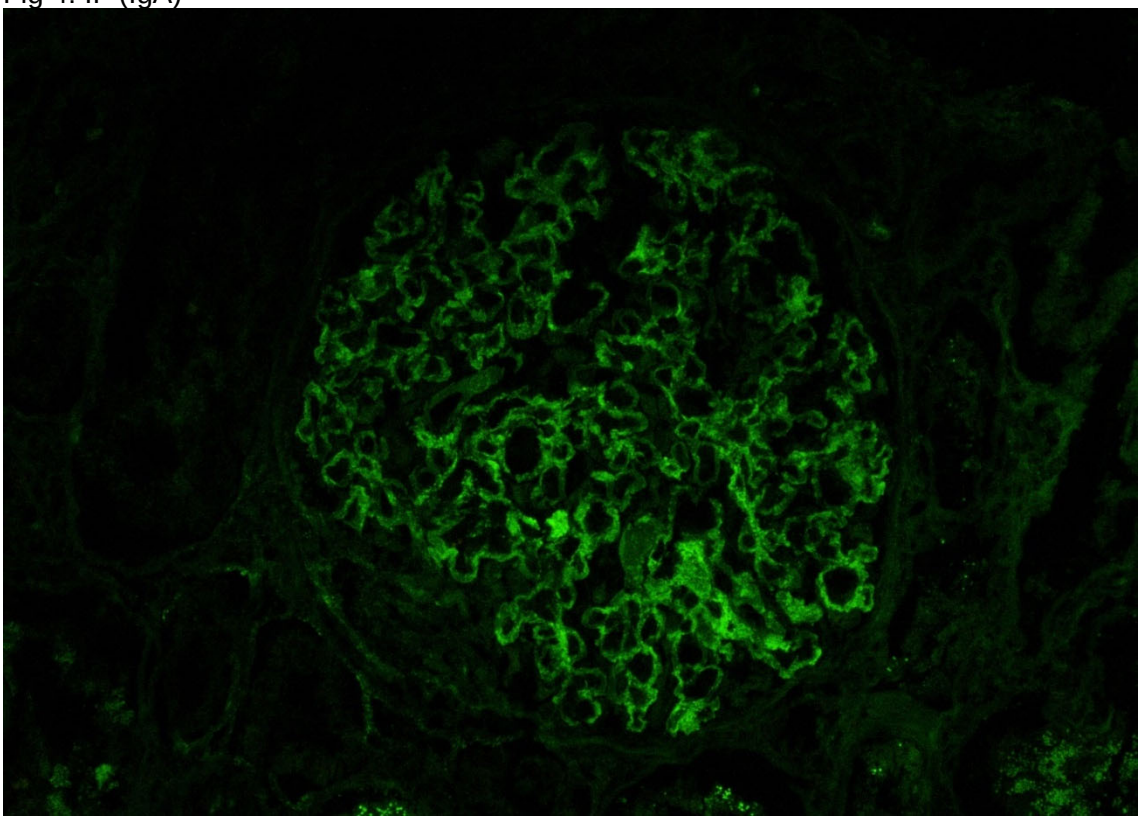

Fig 4: IF (IgM)

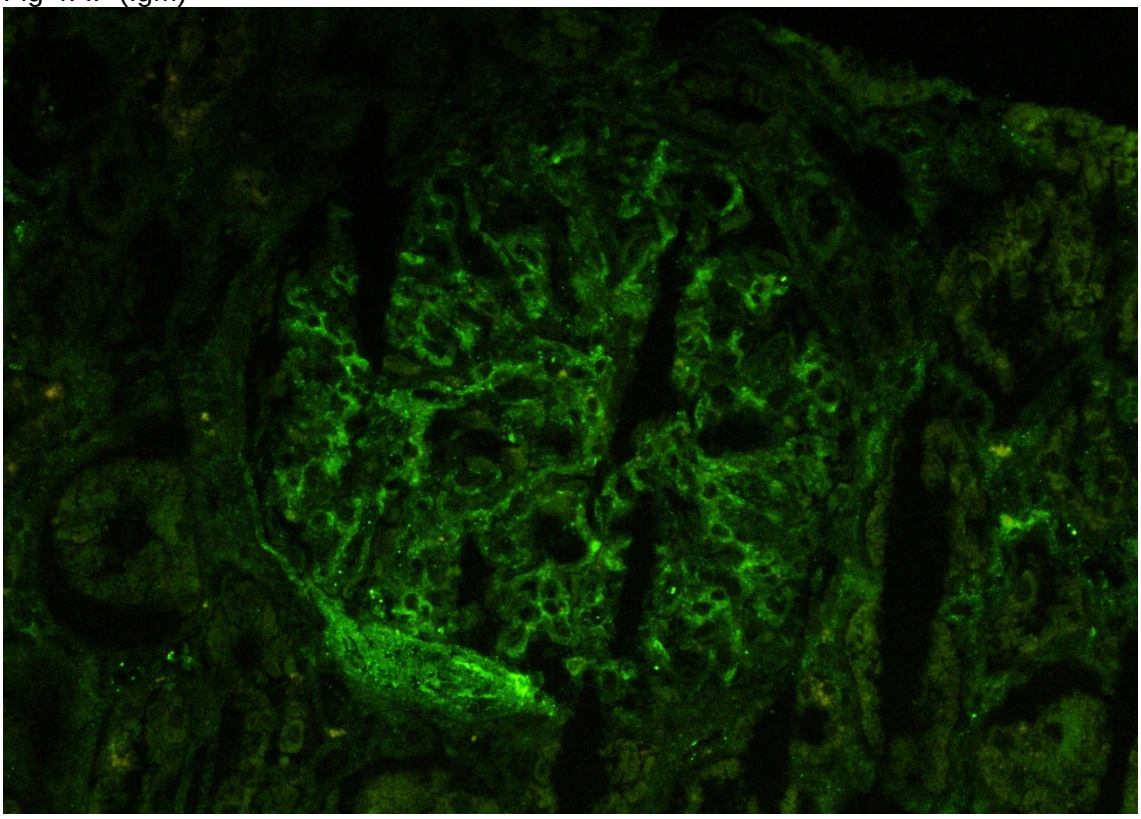

Fig 4: IF (C3)

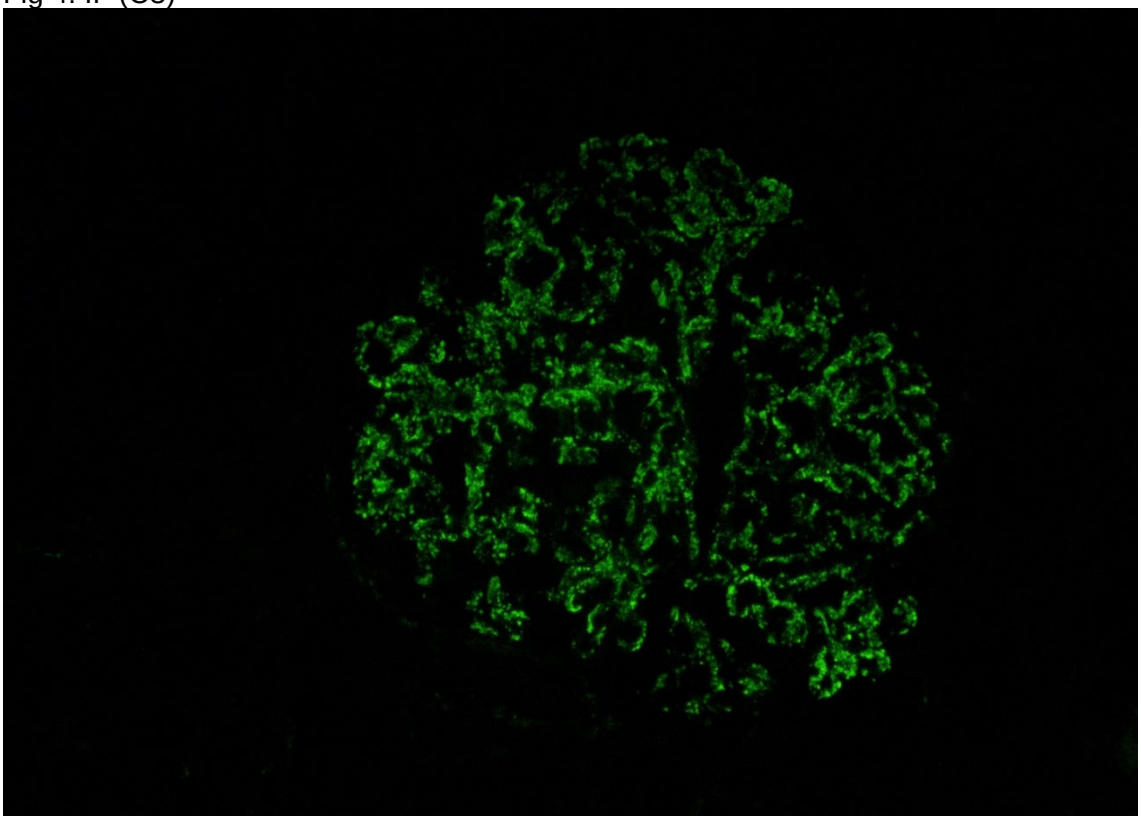

Fig 4: IF (C1q)

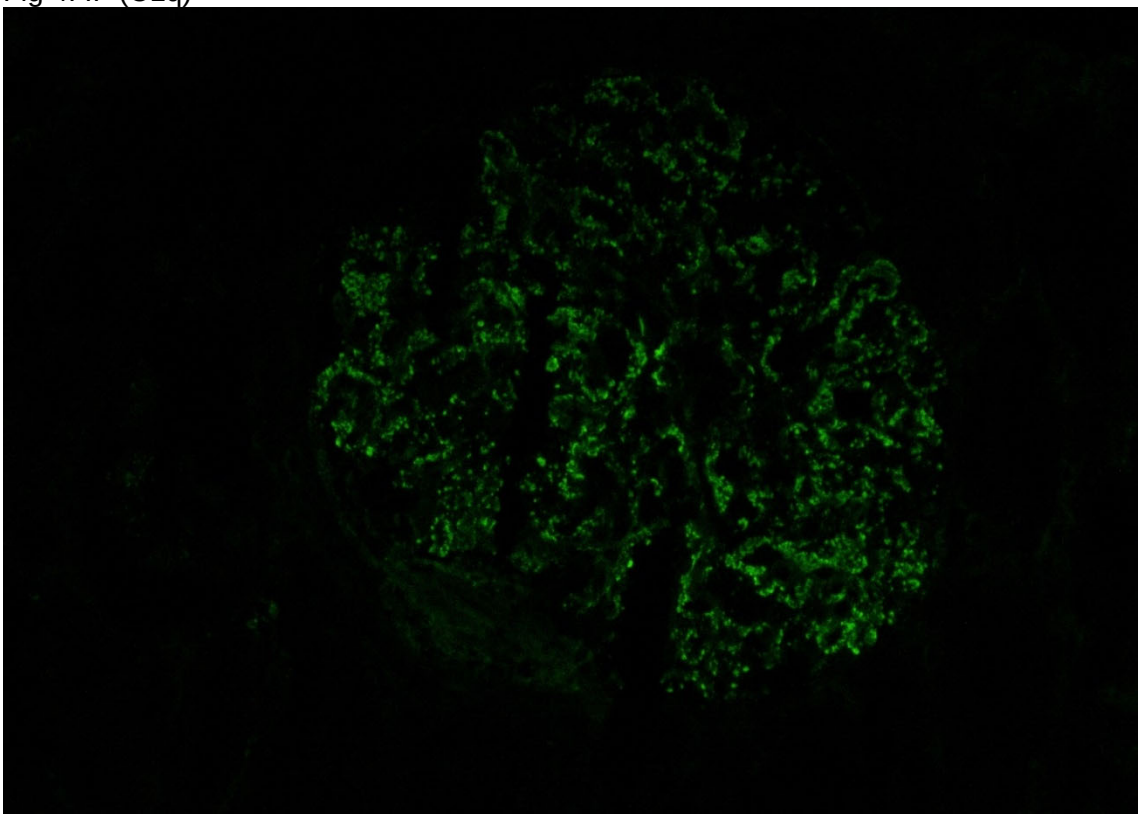

Fig 4: IF (kappa)

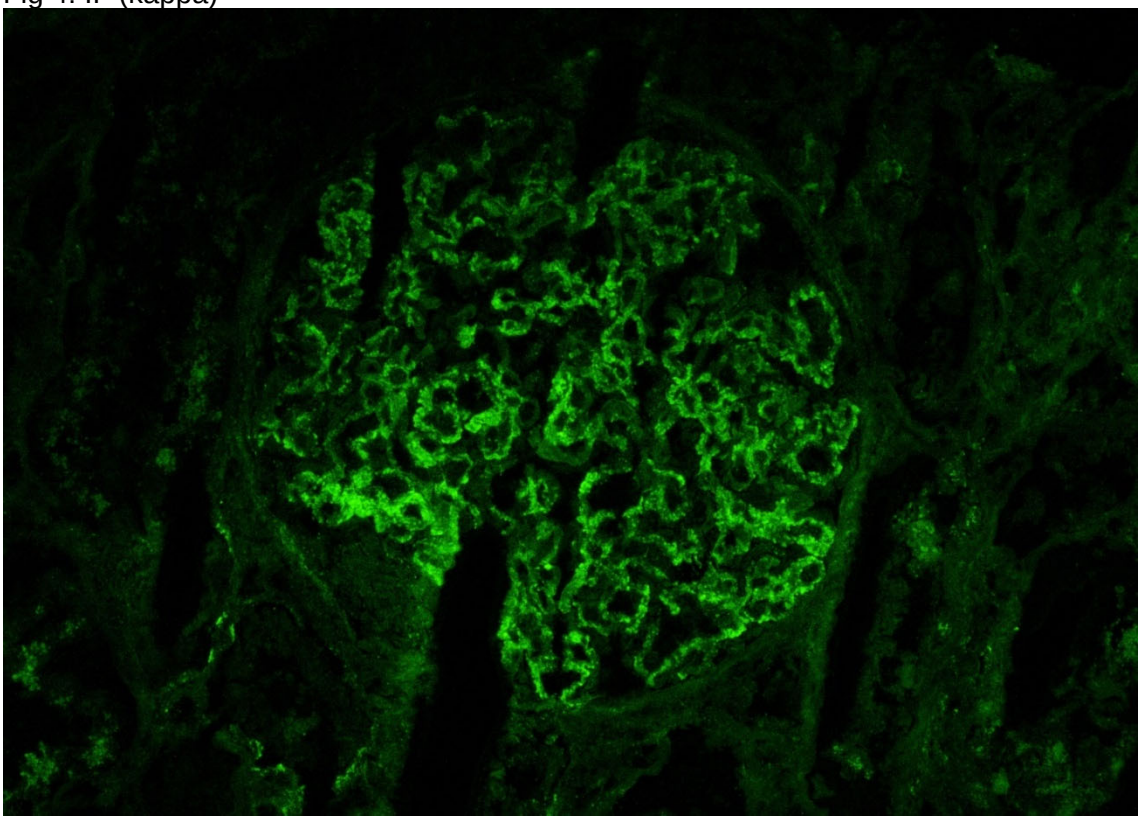

Fig 4: IF (lambda)

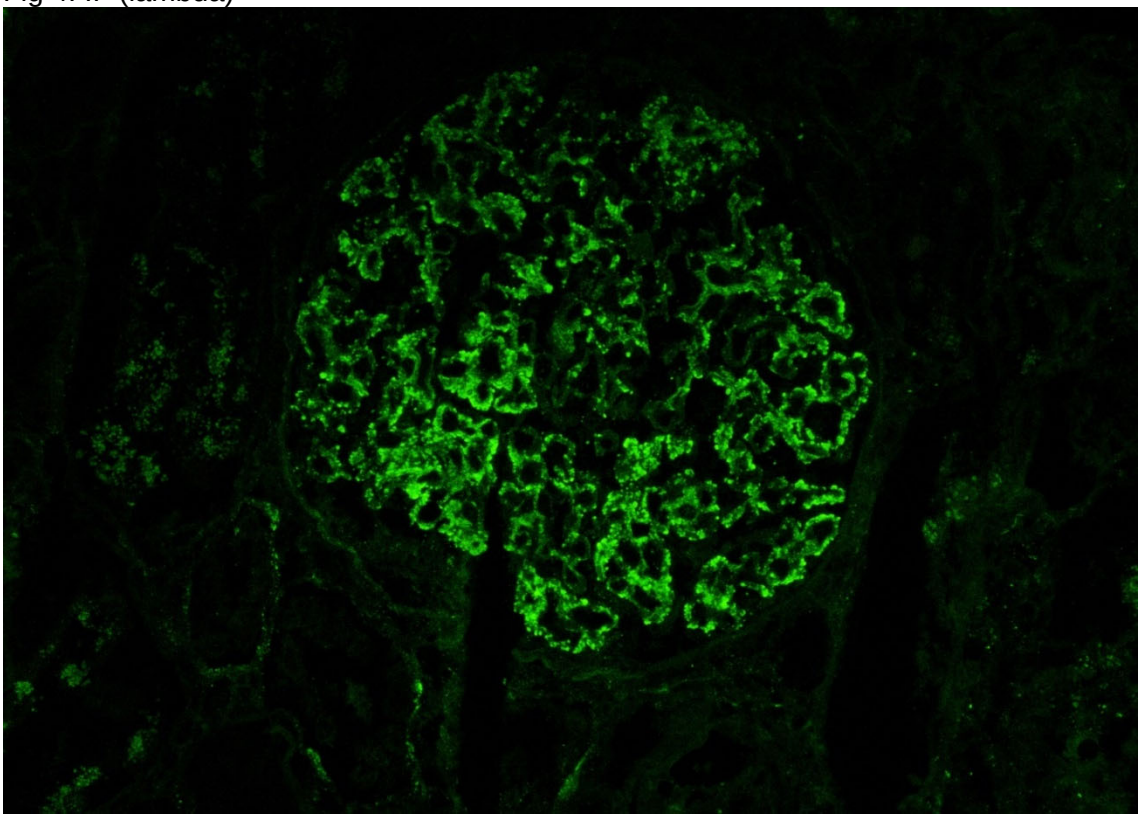

Electron Microscopy (EM):

Fig 5:

Fig 6:

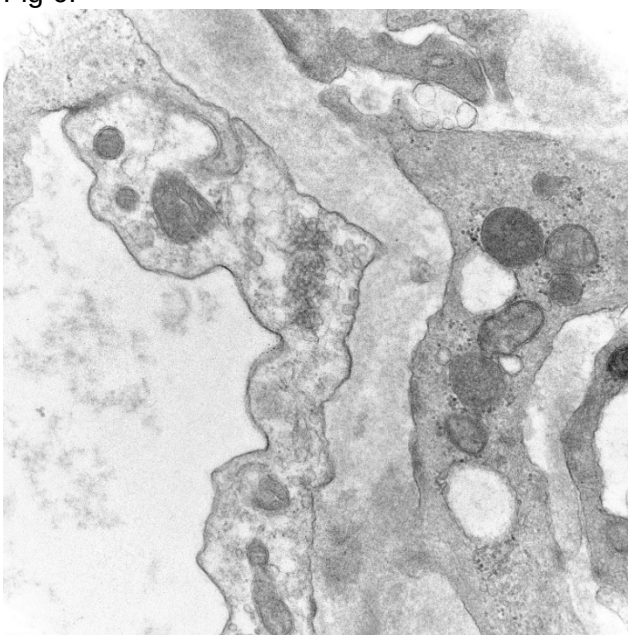

Fig 7:

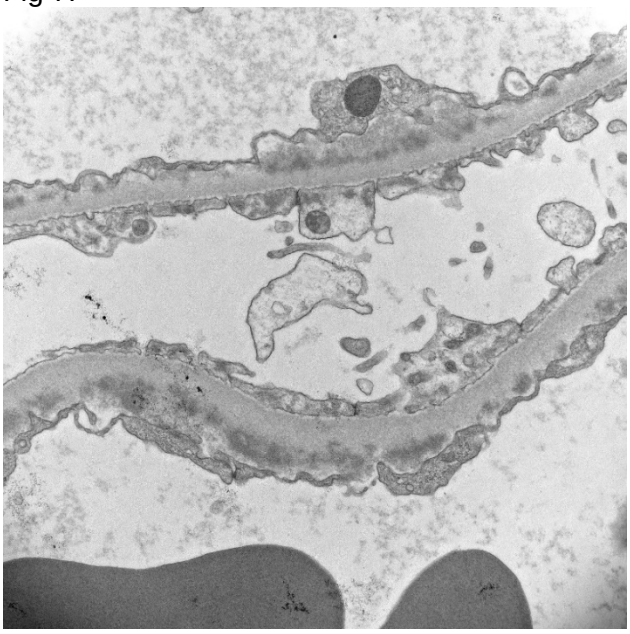

Fig 8:

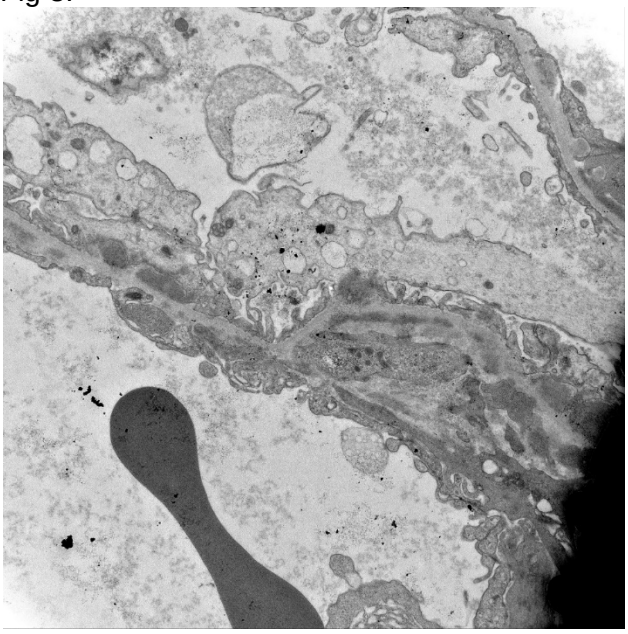

Pathologic Findings

Light Microscopy: The specimen consists of two cores primarily of renal cortex containing approximately 25 glomeruli, of which three are globally sclerotic and three are segmentally sclerosed. Four show cellular crescents, five show segmental endocapillary hypercellularity, and one shows global endocapillary hypercellularity. Glomerular basement membranes (GBMs) appear thickened and double contours are present. Jones stain reveals that more than 50% of the glomeruli show craters/lucencies in their glomerular capillary walls. There is patchy edema and mild to moderate interstitial fibrosis and tubular atrophy. Moderate chronic inflammation accompanies the scarring. Non-atrophic or scarred tubulointerstitium shows minimal mononuclear inflammation. Widespread acute tubular injury is noted. No significant calcification is seen. Arteries show mild intimal sclerosis. Arterioles show mild mural thickening with some hyaline change. No vasculitis is noted.

Immunofluorescence Microscopy: The specimen consists of renal cortex containing approximately 10 glomeruli, of which none are globally sclerotic. There is granular primarily peripheral capillary loop staining for IgG (3+), IgA (2+), IgM (1+) kappa (2+), lambda (2+), C3 (3+) and C1q (2+). 1+ C3 is seen in vessels. Tubular basement membranes and vessels are negative for immune deposits. Albumin and fibrinogen are negative.

Electron Microscopy: The specimen consists of renal cortex containing two glomeruli, of which none are globally sclerotic. Fine structural studies of a single and representative glomerular tuft reveal widespread foot process effacement. Numerous subepithelial electron dense deposits (without overt substructure) are noted. The lamina densa shows reactive type change with some spike formation and areas of lucency. Widespread subendothelial deposits are noted. The mesangial matrix and its cellularity are increased, and numerous mesangial and paramesangial electron dense deposits are present. Tubuloreticular inclusions are seen.

Diagnosis

Immune complex-mediated glomerulopathy with a diffuse proliferative and membranous pattern of injury, suspicious for autoimmune-mediated process/lupus-like nephropathy

Clinical Follow-Up

The patient was treated with pulse steroids with slow taper, hydroxychloroquine, and tacrolimus during the first trimester. Tacrolimus was stopped due to concerns of hyperkalemia, and the patient was started on azathioprine. She had a successful delivery five months later by C-section with AKI during admission attributed to ischemia (no biopsy was performed). After delivery and stopping breastfeeding, she has been on mycophenolate mofetil and tacrolimus. At a recent visit with Rheumatology, she has developed new symmetric arthritis in the small joints of her hands and wrists responsive to methylprednisolone. Serologies remain negative.

Questions for Case 4

1. **What are the glomerular patterns depicted in Fig 3 including insert (Jones)?**

    A. Membranous
    B. Membranoproliferative
    C. Mesangioproliferative
    D. All of the above

    The Jones methamine silver (JMS) stain highlights GBMs and shows spikes and craters/ lucencies, which suggest a membranous pattern of injury. These findings correspond to the EM image in Figure 5, the so-called "spike and dome" pattern. The mesangial nuclei show four or more nuclei and is considered hypercellular, thus mesangioproliferative. There are focal areas of duplication of GBMs in the last JMS image. A normal glomerulus by light microscopy would not show lucencies and spikes, duplication, or mesangial hypercellularity.

2. **In what scenario would you NOT likely see the structure indicated with arrow in Fig 6?**

    A. HIV
    B. Amyloidosis
    C. High interferon states
    D. Lupus nephritis

    The structure seen in Fig 6 is a tubuloreticular inclusion, a distinct intracellular entity often seen within the cytoplasm of endothelial cells. Its presence has been seen in autoimmune diseases such as lupus nephritis and viral infections, and has been shown to be a marker of high interferon-mediated states. Tubuloreticular inclusions have not been associated with amyloidosis of any type.

3. **What is the location of the deposits seen in Fig 7?**

    A. Subepithelial
    B. Mesangial
    C. Subendothelial
    D. No deposits identified

    The location of the deposits in Fig 7 are subendothelial, which correlates with the proliferative pattern of injury seen by light microscopy. The image shows two GBMs only, and no mesangium. Therefore, mesangial deposits can be excluded. The lower one-third of the image shows the capillary loop, identified by fenestrated endothelium at the top, the open capillary loop, and red blood cells within indicating a vascular compartment. On the other side of the lower GBM are podocytes (visceral epithelial cells) that appear extensively effaced.

Discussion

Renal-limited lupus-like nephropathy is characterized by common pathologic findings seen in lupus nephritis, but in the absence of clinical and serological markers indicative of systemic lupus erythematosus (SLE). These biopsy findings include a “full-house pattern” by immunofluorescence and tubuloreticular inclusions by electron microscopy. The relationship between the pathology and the clinical disease process is unclear. Whereas some have suggested that the pathology can precede the clinical manifestations of the disease, others believe it is a stand-alone entity[1].

Pregnancy is commonly known to bring about more flares of lupus. However, active disease may be more tempered as a result of the immunosuppressive effects of pregnancy. Additionally, kidney diseases first identified during pregnancy may present with atypical findings, both clinically and pathologically[1]. In this case, the patient did have hematuria and proteinuria prior to becoming pregnant and was lost to follow-up pre-pregnancy. Thus, it is difficult to determine whether or not she had this kidney disease prior to her pregnancy or if it developed during pregnancy.

In terms of follow-up and prognosis, in one series of four patients with renal-limited lupus-like nephropathy, zero of them developed full clinical signs and symptoms for SLE in the 8-month to 4.5-year follow-up. Additionally, while being treated, one went on to develop CKD Stage 3 in 2.5 years and the others developed ESKD, two of whom received kidney transplantation[2]. Another case series of seven pregnant patients with membranous nephropathy with a full-house pattern found that many had a good prognosis with some going into full remission after delivery. Only one of the seven went on to develop clinical signs and symptoms of SLE[1]. In one study of patients with proliferative lupus-like nephropathy, with the exclusion of those patients going on to develop SLE, 12 adult patients showed variable prognosis, with most undergoing remission at 12 months after initiation of treatment[3]. With variable findings and outcomes, additional research is needed to further characterize the pathology and its prognosis and to understand the clinical disease process.

References

1. Orozco-Guillén AO, Abraham VS, Moguel Gonzalez B, Valdez Ortiz R, Ibarguengoitia F, Del Carmen ZM, Debiec H, Ronco P, Madero M, Piccoli GB. Kidney-Limited Full-House Lupus-like Membranous Nephropathy and Membranoproliferative Glomerulonephritis in Pregnancy. *Kidney Int Rep.* 2023 Jan 16;8(4):932-938. PMID: 37069982.
2. Huerta A, Bomback AS, Liakopoulos V, Palanisamy A, Stokes MB, D'Agati VD, Radhakrishnan J, Markowitz GS, Appel GB. Renal-limited 'lupus-like' nephritis. *Nephrol Dial Transplant.* 2012 Jun;27(6):2337-42. PMID: 22207326.
3. Touzot M, Terrier CS, Faguer S, Masson I, François H, Couzi L, Hummel A, Quellard N, Touchard G, Jourde-Chiche N, Goujon JM, Daugas E; Groupe Coopératif sur le Lupus Rénal (GCLR). Proliferative lupus nephritis in the absence of overt systemic lupus erythematosus: A historical study of 12 adult patients. *Medicine (Baltimore).* 2017 Dec;96(48):e9017. PMID: 29310419.